

THERMAL CHANGES IN AN ARTIFICIAL LAKE SIMULATED USING A
ONE-DIMENSIONAL NUMERICAL MODEL

A THESIS SUBMITTED TO
THE GRADUATE SCHOOL OF NATURAL AND APPLIED SCIENCES
OF
MIDDLE EAST TECHNICAL UNIVERSITY

BY

MEHMET YÜCEL YETGİN

IN PARTIAL FULFILLMENT OF THE REQUIREMENTS
FOR
THE DEGREE OF MASTER OF SCIENCE
IN
CIVIL ENGINEERING

JULY 2017

Approval of the thesis:

**THERMAL CHANGES IN AN ARTIFICIAL LAKE SIMULATED USING A
ONE-DIMENSIONAL NUMERICAL MODEL**

submitted by **MEHMET YÜCEL YETGİN** in partial fulfillment of the requirements
for the degree of **Master of Science in Civil Engineering Department, Middle East
Technical University** by,

Prof. Dr. Gülbin Dural Ünver
Dean, Graduate School of **Natural and Applied Sciences** _____

Prof. Dr. İsmail Özgür Yaman
Head of Department, **Civil Engineering** _____

Asst. Prof. Dr. Talia Ekin Tokyay Sinha
Supervisor, **Civil Engineering Department, METU** _____

Examining Committee Members:

Prof. Dr. Burcu Altan Sakarya
Civil Engineering Dept., METU _____

Asst. Prof. Dr. Talia Ekin Tokyay Sinha
Civil Engineering Dept., METU _____

Asst .Prof. Dr. Cüneyt Baykal
Civil Engineering Dept., METU _____

Asst. Prof. Dr. Melih Çalamak
Civil Engineering Dept., TED University _____

Asst. Prof. Dr. Önder Koçyiğit
Civil Engineering Dept., Gazi University _____

Date: 11.07.2017

I hereby declare that all information in this document has been obtained and presented in accordance with academic rules and ethical conduct. I also declare that, as required by these rules and conduct, I have fully cited and referenced all material and results that are not original to this work.

Name, Last name: Mehmet Yücel YETGİN

Signature:

ABSTRACT

THERMAL CHANGES IN AN ARTIFICIAL LAKE SIMULATED USING A ONE-DIMENSIONAL NUMERICAL MODEL

Yetgin, Mehmet Yücel

M.Sc., Department of Civil Engineering

Supervisor: Asst. Prof. Dr. Talia Ekin Tokyay Sinha

July 2017, 70 pages

This study focuses on release of high temperature water to still water bodies such as lakes and reservoirs. The numerical study is conducted using one dimensional (1D) finite volume code, PROBE. The effect of high temperature water release, effect of wind over the lake in mixture processes, Coriolis' effect and solar radiation effect are investigated numerically using different scenarios that are relevant to such events observed in cooling operations of nuclear power plants. Code validation is performed by reproducing natural stratification in a real lake and formation of a thermocline in summer via calibration of light extinction coefficient, solar radiation and wind velocity. The inflow and outflow of water to and from an artificial lake is studied under several scenarios when a thermal stratification exists. Study shows that 1D model is a viable tool in engineering applications when long term results of water withdrawal and release are required to be assessed in a short time during the cooling operation of aforementioned power plants.

Keywords: PROBE, Thermocline, Nuclear Power Plant Cooling Systems, Light Extinction Coefficient, Solar Radiation

ÖZ

YAPAY BİR GÖLDEKİ TERMAL DEĞİŞİKLİKLERİN BİR BOYUTLU SAYISAL MODEL İLE SİMULASYONU

Yetgin, Mehmet Yücel

Yüksek Lisans, İnşaat Mühendisliği Bölümü
Tez Yöneticisi: Yrd. Doç. Dr. Talia Ekin Tokyay Sinha

Temmuz 2017, 70 sayfa

Bu çalışma yüksek sıcaklıktaki suyun göl gibi akıntısız su kütlelerine verilmesini incelemektedir. Sayısal çalışmada PROBE isimli bir boyutlu (1B) sonlu hacim kodu kullanılmıştır. Yüksek sıcaklıktaki suyun ve rüzgarın göl içindeki karışma süreçlerine etkisi, Coriolis etkisi ve güneş radyasyonu etkisi nükleer santrallerdeki soğutma işlemleriyle alakalı senaryolar üzerinden incelenmiştir. Göldeki mevsimsel doğal tabakalaşmanın ve termoklin formasyonunun sayısal analizinde ışık geçirim katsayısı, güneş radyasyonu ve rüzgar hızı kalibre edilerek gerçek göl ölçüm sonuçlarına ulaşılmıştır. Yapay bir göle su girişinde ve gölden su çıkışında oluşan termal tabakalaşma bir çok durum için çalışılmıştır. Çalışma, 1B modellemenin, bahsi geçen enerji santrallerinin soğutma işlemlerinde su giriş ve çıkışının uzun vadedeki sonuçlarının kısa sürede elde edilmesini gerektiren mühendislik uygulamalarında kullanışlı olduğunu göstermiştir.

Anahtar Kelimeler: PROBE, Termoklin, Nükleer Santral Soğutma Sistemleri, Işık Geçirim Katsayısı, Güneş Radyasyonu

ACKNOWLEDGEMENTS

Firstly, I must express my very profound gratitude to my thesis advisor Asst. Prof. Dr. Talia Ekin Tokyay Sinha for providing me with unfailing support and continuous encouragement throughout my study and during the process of writing of this thesis. This accomplishment would not have been possible without her.

I would also like to thank my manager dear Tuncer Özgüner who gives me full support throughout my graduate studies.

Finally, I would like to thank my fellow officemates for their assistance and encouragement.

TABLE OF CONTENTS

ABSTRACT	v
ÖZ.....	vii
ACKNOWLEDGEMENTS	ix
TABLE OF CONTENTS.....	x
LIST OF FIGURES.....	xii
LIST OF TABLES	xv
CHAPTERS	
1. INTRODUCTION	1
1.1. Scope and Aim of the Current Study.....	5
2. LITERATURE REVIEW	7
2.1. Introduction	7
2.2. Literature on Numerical Studies of Thermal Effects on Lakes.....	10
3. DESCRIPTION OF THE NUMERICAL CODE	13
3.1. Introduction	13
3.2. Basic Assumptions and Brief Descriptions of Governing Equations	16
3.3. Calibration and Use of the Numerical Code	20
3.4. A Typical Case File	22
3.5. Table of Variables Used in Cases of PROBE	26
4. RESULTS.....	29
4.1. Introduction	29
4.1.1. Simplified Shapes of Artificial Lakes	30
4.1.2. Wind Effects on Mixing in a Lake	37

4.1.2.1. Wind Velocity in Single Direction	38
4.1.2.2. Wind Velocity in Two Directions	40
4.1.3. Coriolis' Effect Combined with Wind Effect	43
4.1.4. Turnover Phenomenon.....	47
4.2. Effect of Solar Radiation - Validation of the Code.....	49
4.3. Inflow and Outflow Effects	54
4.3.1. Effect of Location of Outflow and Inflow	54
4.3.2. Effect of Solar Radiation on Combined with Inflow and Outflow Cases	59
4.3.3. Effect of Melted Snow Water as a Surface Inflow	61
5. CONCLUSION	63
5.1. Future Works	64
REFERENCES	65

LIST OF FIGURES

FIGURES

Figure 1.1: An example of thermal stratification (Web 1).	2
Figure 1.2: An example of nuclear power plant built near a water body (Web 2).....	3
Figure 1.3: Typical Inflow and Outflow Mechanism in a Nuclear Power Plant or Industries (Web 3)	4
Figure 1.4: A remotely sensed image showing the effects of thermal pollution (Web 4)	4
Figure 3.1: Schematic Ekman Layer Model	14
Figure 3.2: Flow Chart of PROBE code. (Svensson, 1986)	15
Figure 4.1: Simplified shapes of artificial lake. a) triangular domain, b) rectangular domain c) parabolic domain.....	31
Figure 4.2: Examples of temperature profiles early and late in the season. (Darbyshire and Edwards, 1972).....	32
Figure 4.3: Areal distribution over the vertical for INDARE values of 1 (rectangular), 2 (triangular) and 3 (parabolic).	33
Figure 4.4: Vertical temperature distribution of models.	34
Figure 4.5: Vertical velocity distribution of models.	35
Figure 4.6: a) Google earth view of Llyn Cwellyn. b) Bathymetric map of Llyn Cwellyn. (Darbyshire and Edwards, 1972).....	36
Figure 4.7: Wind effects on mixing in a lake.....	37
Figure 4.8: Schematic of wind blowing in single direction over a triangular cross- sectioned artificial lake.	38
Figure 4.9: Velocity profiles of three different magnitude single direction wind	39
Figure 4.10: Schematic drawing of wind on two directions	40
Figure 4.11: Divided fluxes into two directions without changing magnitude of the resultant.....	41

Figure 4.12: Velocity profiles of (x direction) single and two direction winds	42
Figure 4.13: Vertical velocity profiles in the lake due to same magnitude wind with different velocity components, equal (v2) and unequal (v2_2) distribution on x and y directions.	43
Figure 4.14: The graph of single direction wind (5 km/hr) and Coriolis combined situation: a) U-velocity b) V-Velocity	44
Figure 4.15: Vertical velocity distribution over the water column due to combined effect of two directional wind and Coriolis' effect: a) U-velocity b) V-Velocity	45
Figure 4.16: Coriolis parameters of different locations on earth. (Image is from Google Earth.)	46
Figure 4.17: Velocity profiles under same conditions for different latitudes, hence different f values.	47
Figure 4.18: Vertical Temperature Distribution during Turnover	48
Figure 4.19: Initial profile of temperature within Lake Llyn Cwellyn measured on 30 th of April, 1966. Red squares represent the field measurements, blue line is the profile given as input to the code.....	52
Figure 4.20: An example of sinusoidal variation of short wave radiation in 24 hours given as an input in the code.	53
Figure 4.21: Numerical result (blue line) is compared to the measured field profile of temperature (red squares) in the lake on 3 rd of May, 1966. The initial condition for the run is given in Figure 4.19.....	53
Figure 4.22: Numerical result (blue line) is compared to the measured field profile of temperature (red squares) in the lake on 10 th of August, 1966. The initial condition for the run is given in Figure 4.19.	54
Figure 4.23: Initial temperature distribution without inflow & outflow.....	56
Figure 4.24: Temperature distribution when the inflow at the surface and the outflow at the bottom.	57
Figure 4.25: Temperature distribution when both the inflow and the outflow are at the mid-depth.....	57

Figure 4.26: Temperature distribution when the inflow at the middle and outflow near the bottom.....	58
Figure 4.27: Sinusoidal variation of short wave radiation in 24 hours with two different magnitudes of SRAD: 250 W/m ² & 50 W/m ²	59
Figure 4.28: Temperature distribution when the inflow at the middle and outflow near the bottom combined with different solar radiation magnitudes.	60
Figure 4.29: Temperature distribution when the inflow at the surface and outflow near the bottom combined with 250 W/m ² solar radiation.	61
Figure 4.30: Temperature distribution as the melting water is considered as inflow to the lake.	62

LIST OF TABLES

TABLES

Table 3.1. Variables used in Cases of PROBE.....	26
Table 3.2. Options of variables used in Cases of PROBE.	27
Table 4.1. Historic temperature, rain and sun hour data for Valley, North Wales (Web 5).....	50

CHAPTER 1

INTRODUCTION

Lakes are water bodies, which has different bathymetrical shape and under various external effects such as wind, solar radiation, inflows and outflows. Inflows to a lake could be rain, river or groundwater contributions. Outflow from a lake could be a drain and/or evaporation. Regardless of the fact that there are several natural lakes all over the world; there still exists artificial lakes that are built for different requirements. These requirements could be for instance; agriculture, irrigation, flood control, energy production or cooling systems. In lakes the vertical distribution of temperature is an important research area for engineers, ecologists and geomorphologists. In literature it has been abundantly stated that the vertical temperature distribution in a lake depends on wind effects, solar radiation, seasonal heating/cooling and inflow/outflows (Darbyshire and Edwards, 1972; Spiegel and Imberger, 1980; Horne and Goldman, 1994). One of the main driver of mixing in a lake is the wind stress on the surface of the lake. The shear stress due to wind causes a rotational movement in the lake. Seasonal heating and cooling causes a thermal stratification in a lake. Normally, in north hemisphere, in summer, the lakes divided in three horizontal layers which the upper layer is epilimnion, the bottom zone is hypolimnion and the middle zone is metalimnion. Schematic of such stratified lake is given in Figure 1.1.

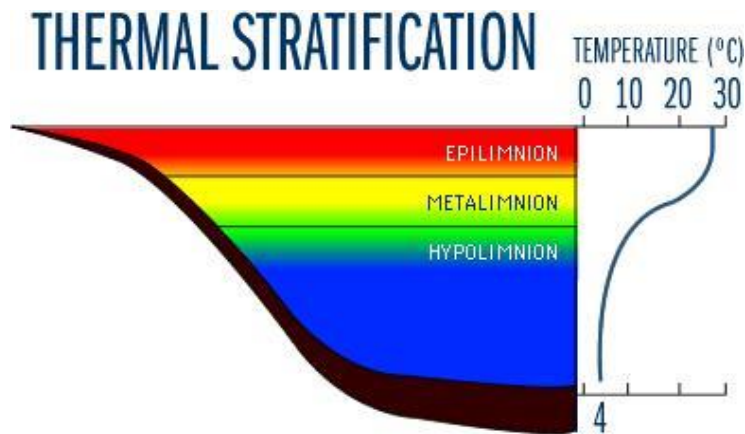


Figure 1.1: An example of thermal stratification (Web 1).

The depth of these layers depend on external effects and geomorphological properties of the lake. In spring and autumn, generally no stratification occur which means the temperature is almost same at every location and the lake is thermally well-mixed. In winter, if ice occurs on the surface of the lake, it prevents water mixing by stopping the shear force of the wind.

In this study, an artificial lake is taken into consideration to discuss the effect of several external parameters in vertical temperature distribution within the water body. Numerical model used for the parametric study is validated using real data of Lake Llyn Cwellyn in North Wales (Darbyshire and Edwards, 1972). Effect of several external factors are also discussed in Chapter 4 in case the artificial lake is used as cooling reservoir of a nuclear power plant.

Figure 1.2 illustrates The Doel nuclear power station which is located on the bank of the Scheldt river, Belgium. All nuclear power plants are often built near a water body if exists. Otherwise, a man-made lake at necessary dimensions should be built.



Figure 1.2: An example of nuclear power plant built near a water body (Web 2).

The most crucial parts that require attention when building a nuclear power plant is the outflow of the hot water from nuclear power plant and withdrawal of cold water from the lake. These cause rapid changes on the vertical temperature distribution. The temperature of the released water is often expected to abide with relevant specification from environmental agencies. In Figure 1.3, a typical inflow and outflow mechanism in a nuclear power plant or industry is shown.

Figure 1.4 shows effects of thermal pollution by using thermal photographic technology in Maasvlakte Project, near city of Rotterdam, Netherlands. In Figure 1.4, red colour and orange colour represent the hottest water and hot water, respectively. Green, magenta and dark blue colours represent water getting colder. The reason for dark blue colour at the exit of the plant is due to existence of an effluent pipeline at that location in the system, where thermal imaging only captures the temperature of the pipeline but not the temperature of pipe's content.

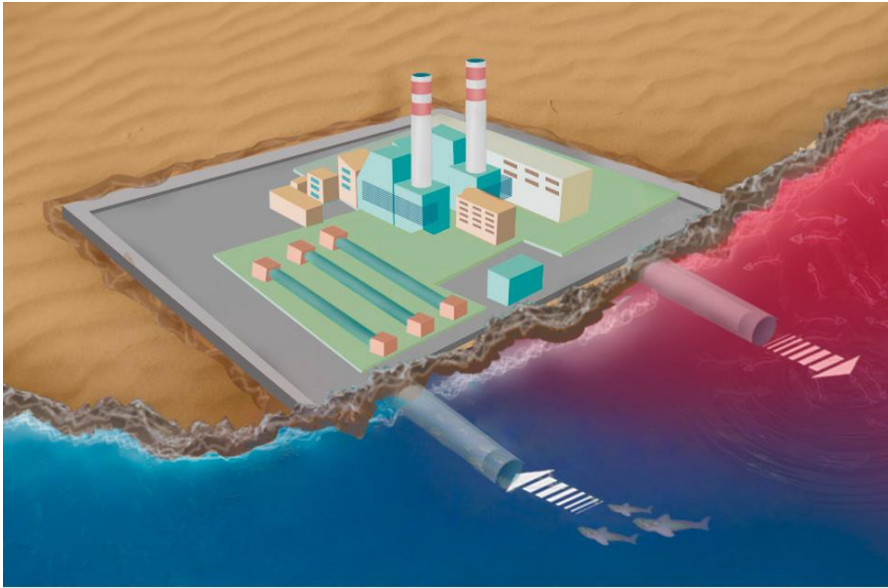


Figure 1.3: Typical Inflow and Outflow Mechanism in a Nuclear Power Plant or Industries (Web 3)

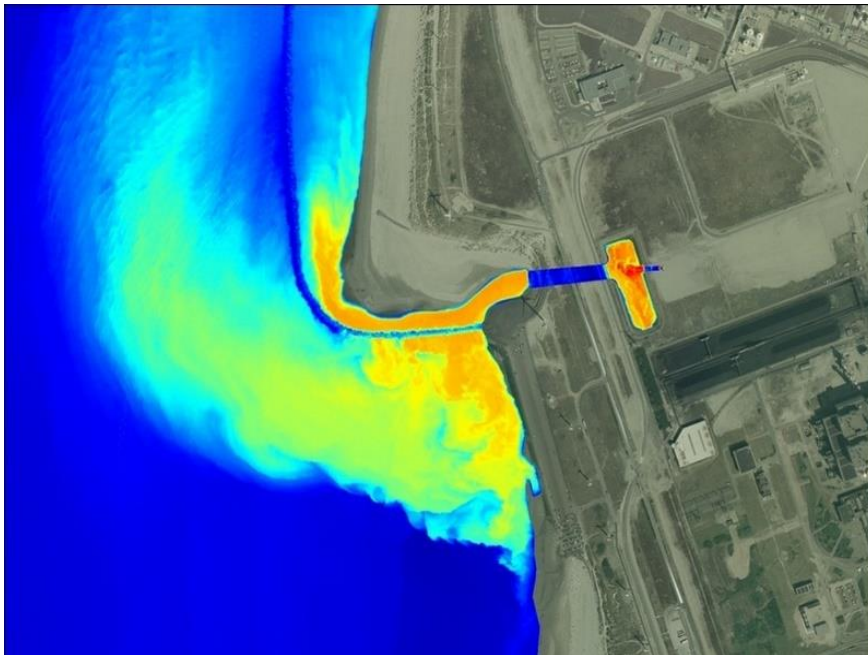


Figure 1.4: A remotely sensed image showing the effects of thermal pollution (Web 4)

1.1. Scope and Aim of the Current Study

The aim of the study is to identify the effects of possible scenarios on water temperature over a simplified lake geometry using one-dimensional numerical modelling. Program for Boundary Layers in the Environment (PROBE) is the numerical program based on Fortran, used in this study to simulate different cases. The code is based on the original work of Svensson (1978) and frequently used by Swedish Meteorological and Hydrological Institute (SMHI) on several projects. More information and the code could be obtained through SMHI. This study concentrates on understanding the effects of wind velocity, Coriolis' effect, inflow and outflow and solar radiation on lake water temperature. The motivation of this study can be explained as;

- Certain scenarios can guide the operation of a real life power plant or an industry that is located near a lake.
- Scale effects might hamper the results of the laboratory experiments of such phenomenon.
- Numerical modelling has the advantage of elimination of these scale effects.
- The one-dimensional modelling is much faster therefore, many different scenarios can be tested. One dimension is actually the z-axis, namely; the vertical distribution of variables are considered in this study.

Calibration of the code for different cases has crucial importance. Among many other parameters, by changing wind velocity, time step and light extinction coefficient of the lake quiet reasonable results can be reached. Calibration requires field measurements of many variables such as wind, solar radiation, vertical temperature distribution in the lake.

Once the calibration of the 1D code is done for the location of interest, it could easily be employed for engineering applications such as determination of long term effects of water withdrawal and/or solar radiation on thermal conditions in lakes used for

cooling systems of nuclear power plants. One such application in near future is possible for Akkuyu Plant planned to be built in Turkey.

CHAPTER 2

LITERATURE REVIEW

2.1. Introduction

Even though classified as still water in certain fluid mechanics applications, the fluid motion in lakes is quite complex. This makes physical system of a lake, similar to oceans and atmosphere, very diverse. Lakes also come in various shapes and sizes, and this causes complex boundary effects. Winds induce currents, density differences over the depth is possible due to temperature differences, concentration might vary inside a lake due to dissolved matter (Imboden and Wüest, 1995).

Mixing mechanisms in lakes are of particular interest for civil and environmental engineers, biologists and ecologists, and even of nuclear engineers, specifically if the lake is used as a cooling water supply to a nuclear facility.

Mixing in lakes and reservoirs is typically related to stratification in the water body. Stratification is often due to temperature variation. Temperature variation affects the overall energy balance inside the lake

Socolofsky and Jirka (2004) define wind as the major external input responsible for mixing. Potential energy of a lake gets restructure as the wind adds kinetic energy to the lake system. Wind affects the lake through the shear it imparts on the water surface.

Spiegel and Imberger (1980) showed that wind stress active on a stratified lake causes large-scale motions such as circulation and waves. The wind also stirs the surface waters to form a turbulent, well-mixed layer -the epilimnion- which depends as colder water from the hypolimnion is entrained into epilimnion. They suggest the incorporation of turbulent kinetic energy production in momentum equation in one-dimensional models to produce the accurate effect of wind on the lakes in numerical modelling.

Boehrer and Schultze (2008) suggest that density differences in water bodies affect the evolution of chemicals inside, which in return affect the living organisms in lakes. They point out that temperature and dissolved substances contribute to density differences in water. In warm seasons in deep lakes thermal stratification could be observed and during cold seasons the surface cooling might force vertical circulation of water masses, such that some lakes might experience full overturns. With incoming solar radiation surface water heats up and with mechanical energy coming from wind, warmer but less dense water is mixed upto a limited depth. They observed that in sufficiently deep lakes, thermal stratification holds until cooler autumn and winter temperatures force a circulation into deep waters. As defined in the literature, the warm surface water layer, epilimnion, and cold layer called hypolimnion, is connected by a zone with sharp temperature variation, which is referred as thermocline.

Study of Socolofsky and Jirka (2004) explained that a thermocline develops depending on mixing action of the wind and the penetration depth of the solar radiation. Thermocline is accompanied by a density gradient.

In the study of Darbyshire and Edwards (1972) it is stated that a thermocline forms not only with an input of heat but also an intake of mechanical energy as work. This mechanical energy has to be done against gravity as the warmer lighter water replaces the colder denser water. The heat input could come from conduction if the air temperature is higher than the water temperature or it could directly come from solar

radiation. They stated that the second effect is much more prominent and the first can be ignored in comparison.

In literature there exists several studies that measures the local solar radiation. Few examples to such studies in Turkey are by Çağlar et al. (2012) and Aksoy (2011). These studies could provide important input required by numerical model in lake studies.

According to Tucker and Green (1977), the lake size is in direct correlation with the depth of the summer thermocline. They also used the assumption in their study that solar heating decays exponentially with depth with a scale length of β^{-1} , where β is defined as an extinction coefficient for the solar heat.

Kirillin and Shatwell (2016) discuss the effect of transparency of the lake as a factor in penetration of the solar radiation. Decreased transparency for example reduces the penetration of solar radiation to deeper layers, which decreases deep water temperatures and increases vertical temperature gradients and water column stability. Accordingly, transparency can have large effects on stratification duration in some lakes.

Kraus and Turner (1967) concluded that the convective mixing resulting from penetrative radiation has a rate of the same order as that produced by mechanical stirring. They stated that during the summer the radiation effect is likely to be predominant.

Socolofsky and Jirka (2004) list the processes that activates the mixing in a lake or reservoir are driven by diurnal (daily) forcing, such as by wind, inflows and outflows, radiation exchange, and chemistry.

These processes could be observed in-situ in a lake as most often discussed in the literature, could be physically modelled in the laboratories or could be numerically modelled.

2.2. Literature on Numerical Studies of Thermal Effects on Lakes

Sahlberg and Persson (2010) explain that modelling studies play a key role in exploring the processes responsible for changes in lakes. They claim that as vertical gradients in lakes are larger than gradients in the horizontal, the short computation time and associated potential for multiple runs offered by a one-dimensional model is advantageous. They used PROBE in their study. This code has previously been used to model the thermal changes and mixing processes in several European lakes. They said in their study that “Results from these simulations showed there was a good agreement between the modelled and measured temperatures. Overall, the closeness of fit of modelled and observed data confirms the suitability of the PROBE model for simulating these lakes and provides a robust way of exploring their response to future changes in the climate.”

PROBE has been widely used over the years in many different studies. Elliot et al. (2006) used the code for modelling phytoplanktons in Lake Erken, Omsted and Svensson (1984) used the same code for modelling ice formation. Sahlberg (1983) used an earlier version to simulate cooling in Lake Varmon. Omsted et al. (2005) applied PROBE to Baltic Sea in order to forecast temperature in the sea.

Owens (1998) used a hydrothermal model based on the conservation equations for heat, water volume and in the case of the multi-lateral model, turbulent kinetic energy to study the thermal conditions of Cannonsville Reservoir. In his model the one-dimensional equations assume that temperature, vertical water motion and mixing are uniform in the horizontal plane and vary only in the vertical direction and over time.

Hamilton and Schladow (1997) stated that in ecological water quality models, the continuously stirred or two-layer vertical system approaches for water bodies is an oversimplification of transport and mixing processes in a water body. MacIntyre et al. (1999) studied the nutrient mixing in Lake Mono in California by applying a one-dimensional model. Based on their results, the upward flux of nutrients was believed

to occur via mixing in turbulent eddies. Based on the study of Yeates (2008) on deep mixing in stratified lakes and reservoirs, different turbulence quantities could characterize the formation of an Ekman Layer in water bodies in the presence of wind shear on the free surface. Ekman layer is the layer of fluid where surface stress, Coriolis and pressure gradients act to create a spiralling motion within the water column. This is similar to the findings of Svensson (1979). Both studies showed that turbulence should be considered in lake motion as it could affect the shear stress distribution within the lake. As stated by Quay et al. (1980) a geochemical study of a natural water system often requires estimates of turbulent transport in an equation describing the rate of change of a concentration field with time as water motions are variable in time and space.

Romero et al. (2004) used one- and three-dimensional (3D) modelling on two different reservoirs to observe some biogeochemical processes. The one-dimensional model shows similarities to PROBE. The one-dimensional hydrodynamic model called DYRESM was used to simulate the temperature, salinity, and density in lakes and reservoirs, while a three-dimensional model, ELCOM was used to observe internal waves in lakes and floods in reservoirs. They stated that flow dynamics related to movement of particles, mixing and settling of nutrients during floods and similar complex flow related phenomena requires 3D modelling.

In the study of Sahlberg (2003), the thermal structure of lake Akkajaure is presented. He stated in his work that the quality of a model is judged by its ability to reproduce the temperature profiles measured in the reservoir.

Perroud et al. (2009) evaluated the suitability of one-dimensional lake models to reproduce the evolution of water temperature profiles in the deep perialpine Lake Geneva. Even though there exists some controversy regarding the application of one-dimensional models to large and deep lakes, as the atmospheric conditions are heterogeneous over the large water surface areas, and horizontal advection is

neglected, after slight calibration their model predicted seasonal evolution of water temperature profiles with reasonable accuracy in Lake Geneva.

Gal et al. (2003) simulated the thermal dynamics of Lake Kinneret using one-dimensional DYRESM. The simulations extend over a period of 45 months. They self-criticized their use of constant light extinction coefficient throughout the year, nevertheless, concluded that the code was capable to capture the physics inside the lake.

In the literature it is commonly accepted that extinction coefficient is a key parameter in determining the thermal changes in a lake. Even though results of Persson and Jones (2008) suggested that, larger extinction coefficients initially led to surface waters becoming warmer many other studies have shown that an increase in the extinction coefficient leads to a reduction in mixed depth. (Kling, 1988; Mazumder et al., 1990; Mazumder & Taylor, 1994; Schindler et al., 1996; Yan & Dillon, 2000), as well as a reduction in the heat content of lakes (Hambright, 1994; Hocking & Straskraba, 1999; Jones et al. 2005).

In recent years in Turkey few important studies have been conducted on lakes and their thermal characteristics. One such study is by Çalışkan and Elçi (2009). They used quasi-3D Environmental Fluid Dynamics Code, EFDC, to model the hydrodynamic configuration of Tahtalı reservoir. They discussed the relation of location of the water removal outlet to the improvement of water quality in the reservoir. Using the model, they tested four different outlet locations, which result in different temperature profiles and different mixing processes in Tahtalı reservoir.

CHAPTER 3

DESCRIPTION OF THE NUMERICAL CODE

3.1. Introduction

PROBE is the acronym for “Program for Boundary Layers in the Environment”. It is the numerical code used in the thesis study. It is a one-dimensional (1D) finite volume code. The code is originally written by Urban Svensson in 1978. (The Swedish Meteorological and Hydrological Institute S-601 76 Norrköping, Sweden)

PROBE is a Fortran based program, which solves equations of one-dimensional transients. The Ekman layer is a typical example of boundary layer that this code is capable of simulating. As shown in Figure 3.1 in an Ekman layer surface stress decreases away from surface to deeper section of oceans/lakes. The main reason of this decay is the Coriolis’ effect.

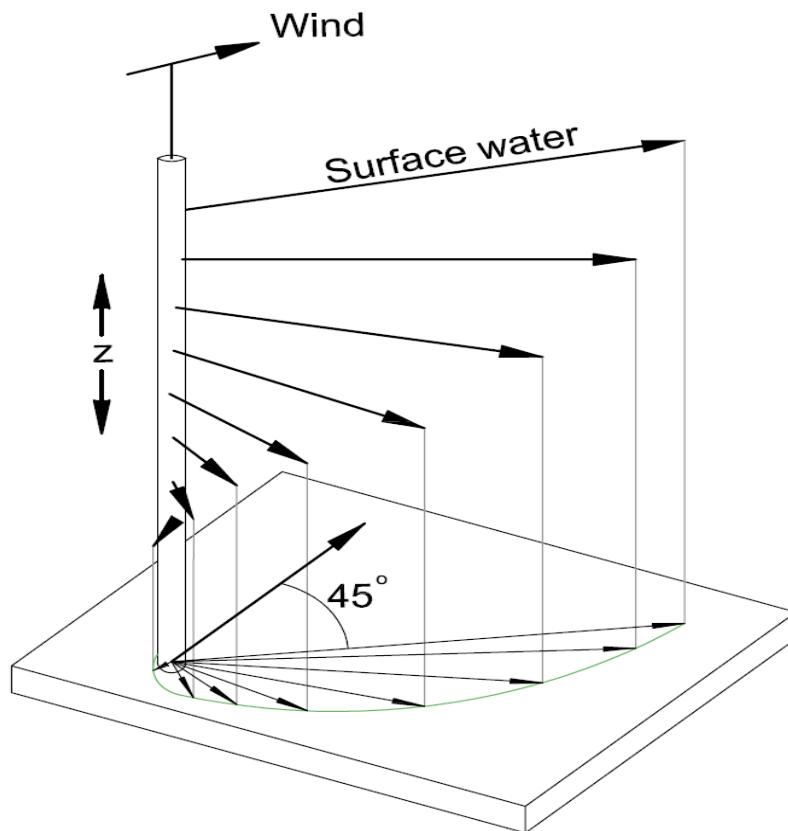


Figure 3.1: Schematic Ekman Layer Model

The basic complexity in these kinds of flows is the characterization of the turbulent mixing in mathematical terms. PROBE uses $k-\varepsilon$ model to calculate mixing coefficients and hydrodynamics of the flow. It solves two momentum and continuity equations. Besides, additional variables can be considered such as upto four scalar concentrations, heat energy and salinity. In order to avoid any aberration in the source code and to enable user friendly usage of PROBE, the subroutine called "CASE" has been structured and it is expected from user to only modify this file. All units are in SI system. The details of a typical case file of the present study is presented later in this chapter.

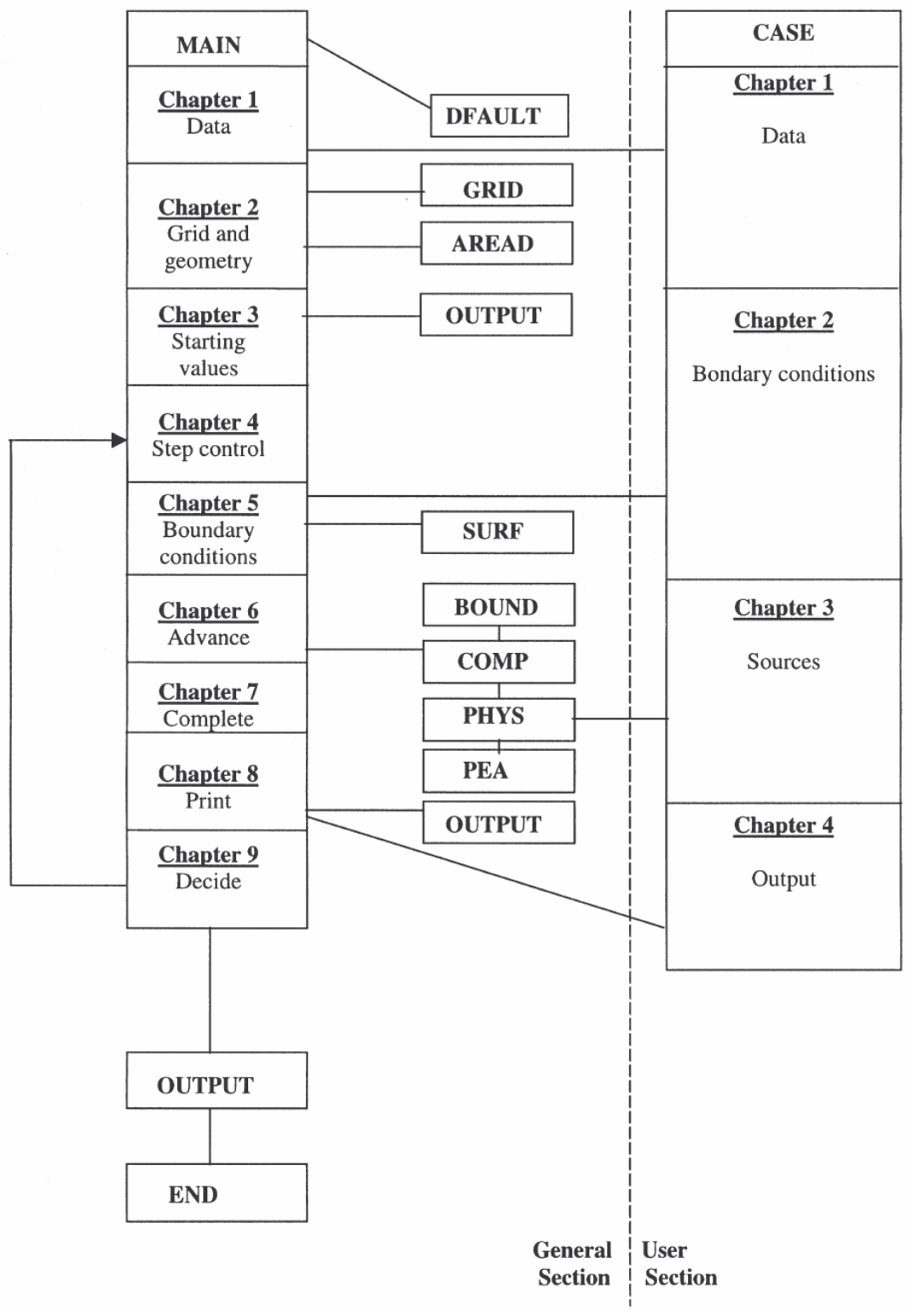


Figure 3.2: Flow Chart of PROBE code. (Svensson, 1986)

There are several application areas of PROBE. For environmental flows an idealised one-dimensional model could provide a good approach and helpful insight in understanding the problem.

3.2. Basic Assumptions and Brief Descriptions of Governing Equations

In the code, all gradients in the horizontal directions are neglected. So effect of horizontal distribution of heat and momentum fluxes at the lake surface is not possible to include. Turbulent mixing processes can be described by turbulent exchange coefficients. This description is based on Reynolds Averaging of Navier-Stokes Equations (RANS). Internal absorption of short wave radiation is assumed to follow an exponential decay law. Gravitational effects are assumed to obey the Boussinesq approximation. Effect of the rotation of the Earth is described by the Coriolis’ parameter, *f*. Adjective momentum transport across the boundaries is not allowed.

❖ All differential equations governing the PROBE could be written in the form of;

$$\frac{\partial \phi}{\partial t} = \frac{\partial}{\partial z} \left(\Gamma_{\phi} \frac{\partial \phi}{\partial z} \right) + S_{\phi} \dots\dots\dots (1)$$

Simply, Equation 1 shows that change in time is related to diffusion and presence of source/sink. Here, ϕ is the dependent variable, *t* is time, *z* is the vertical coordinate, *x* is the horizontal coordinate, *u* is the horizontal velocity, Γ_{ϕ} is the exchange coefficient, and S_{ϕ} is the source and/or sink terms.

❖ Momentum Equations are;

$$\frac{\partial(\rho u)}{\partial t} = -\frac{\partial p}{\partial x} + \frac{\partial}{\partial z} \left(v_{eff} \frac{\partial(\rho u)}{\partial z} \right) + f \rho v \dots\dots\dots (2)$$

$$\frac{\partial(\rho v)}{\partial t} = -\frac{\partial p}{\partial y} + \frac{\partial}{\partial z} \left(v_{eff} \frac{\partial(\rho v)}{\partial z} \right) - f \rho u \dots\dots\dots (3)$$

where t is time coordinate, x and y are the horizontal space coordinates, z is the vertical space coordinate, u and v are horizontal velocities in the x - and y -directions, respectively, p is the pressure, f is the Coriolis' parameter, and ρ is the density. The kinematic effective viscosity, ν_{eff} , is the sum of the turbulent viscosity, ν_τ , and the laminar viscosity, ν . There are several ways to treat pressure gradient terms, depending on the problem considered;

i. Prescribed

In the prescribed treatment of pressure, the $\frac{dP}{dx}$ or $\frac{dP}{dy}$ values are taken as constants directly given by the user.

ii. By using total mass flux with the formula below

$$\frac{\partial p^{i+1}}{\partial x} = \frac{\partial p^i}{\partial x} + PFILT \times (\overline{\rho u} - \overline{\rho u_p}) \dots\dots\dots (4)$$

where i is iteration step, $PFILT$ is a constant, ρu total mass flux and ρu_p prescribed total mass flux. Value of $PFILT$ will not affect the converged solution. It just affects how fast the convergence occurs and the readjustment of the pressure field based on the observed mass fluxes in other words by applying conservation of mass.

iii. The last way is the pressure formula for lakes and reservoirs derived by Svensson (1978)

$$\frac{\partial}{\partial t} \left(\frac{\partial p}{\partial x} \right) = \rho g \frac{\pi^2 \bar{u} \times D}{L_x^2} \dots\dots\dots (5)$$

$$\frac{\partial}{\partial t} \left(\frac{\partial p}{\partial y} \right) = \rho g \frac{\pi^2 \bar{v} \times D}{L_y^2} \dots\dots\dots (6)$$

where g is the acceleration due to gravity, D is the depth, and L_x and L_y are horizontal dimensions of the water body. In the CASE file these options for pressure treatment can be expressed using indices called INDPX and INDPY values. Please see Subsection 3.5 for possible options.

❖ Heat Energy Equation is given by;

$$\frac{\partial}{\partial t}(\rho c_p T) = \frac{\partial}{\partial z} \left(v'_{eff} \frac{\partial}{\partial z} (\rho c_p T) \right) + R(1 - \eta)e^{-\beta(D-z)} \quad \dots\dots\dots (7)$$

where temperature is denoted by T , c_p is specific heat, v'_{eff} is the sum of the eddy diffusivity v_t' and the laminar diffusivity for heat, R is incoming short wave radiation, η is the fraction of R absorbed at surface, and β is the extinction coefficient.

❖ Salinity and Concentration Equations

The code has capability to handle upto 4 different concentrations of a constituent and salinity, separately. However in this study, salinity and other dissolved concentration are not taken into consideration.

❖ Turbulence Model

PROBE has two different models such as single-equation k model and two-equation k-ε model. In k model kinematic eddy viscosity and kinematic eddy diffusivity are calculated using turbulent kinetic energy and turbulent length scale. In k-ε model, the dynamical eddy viscosity and kinematic eddy diffusivity, λ are calculated from the turbulent kinetic energy, k , and its dissipation rate, ϵ . In the below equations c_μ values are empirical constants. The default values of these constants in the original source code remain unchanged in the current study.

$$\nu_T = C_\mu (C_\mu^0)^3 \frac{k^2}{\varepsilon} \dots\dots\dots (8)$$

$$\lambda_T = C'_\mu (C_\mu^0)^3 \frac{k^2}{\varepsilon} \dots\dots\dots (9)$$

❖ Turbulent Prandtl / Schmidt numbers

In the code there are two option available for the turbulent Prandtl / Schmidt numbers. The numbers can be given as constant values or they could be calculated by using formula below,

$$\sigma = \frac{\phi}{\phi_T} \times \frac{1 + \phi'_T (c'_T - \phi_T) B}{1 + B \phi \phi_T} \dots\dots\dots (10)$$

where

$$B = g \frac{k^2}{\varepsilon^2} \left[2\alpha(T - T_0) \frac{\partial T}{\partial z} - \alpha_s - \alpha_{c_1} \frac{\partial C_1}{\partial z} \dots \alpha_{c_4} \frac{\partial C_4}{\partial z} \right] \dots\dots\dots (11)$$

B is a buoyancy parameter.

❖ Boundary Conditions

For momentum, heat energy, salinity, and concentrations, boundary conditions can be applied in two different ways; either the flux of the variable or the value of the variable at the boundary is given. A shear stress at a water surface, for example, is a "flux condition", while the zero velocity at a bottom is a "value condition".

The boundary conditions for k and ε are somewhat different. When a shear stress or a turbulence producing buoyancy flux is present at a boundary, k and ε are specified close to the boundary in relation to these fluxes. If no shear or buoyancy flux is present, k and ε are treated as if the boundary was a symmetry plane, i.e. a zero gradient condition is assumed.

❖ Equation of state

According to the equation of state there is a quadratic relationship between temperature and density and a linear relationship for salinity and concentrations.

$$\rho = \rho_0(1 - \alpha_1(T - T_r)^2 + \alpha_2S + \alpha_3C_1 + \alpha_4C_2 + \alpha_5C_3 + \alpha_6C_4) \quad \dots\dots\dots (12)$$

where ρ_0 is a reference density, T_r is the temperature of maximum density and α_1 - α_6 are coefficients. In this study the equation above is transformed into below equation by eliminating salinity and concentrations.

$$\rho = \rho_0(1 - \alpha_1(T - T_r)^2) \quad \dots\dots\dots (13)$$

3.3. Calibration and Use of the Numerical Code

In order to use PROBE in this study, the capability of the code to produce a real case is tested by calibrating it. After calibration, which is discussed in Results chapter in detail, the code is observed to produce reasonable results. After the validation, several scenarios have applied to an artificial lake. In some cases time step is needed to be taken much smaller. The time step is called TFRAC in this code. TLAST represents the maximum simulation time and it is equal or more than the multiplied values of LSTEP and TFRAC, where LSTEP shows the number of time steps needed.

In the code, the variable INDARE indicates the cross section type of the reservoir. If the cross section of the artificial lake is triangular as in this study, INDARE could be taken equal to 2. Coriolis' parameter can be directly entered by using CORI variable. Wind effects could be entered by using momentum flux values. In PROBE, FLUXHZ (J) is for surface wind effects. For U direction winds J is equal to 1 and for V direction winds J is equal to 2. This is simply a flux calculated as density of air times the velocity of air, ρ_u or ρ_v . Effect of surface wind will further be discussed in Chapter 4.

As indicated in the “Literature Review” section the extinction coefficient is important in understanding the heat content of a lake. Variable BETA in the code is defined as the extinction coefficient. BETA has crucial effects on thermocline and solar radiation cases. The penetration of the sun light is directly related to this parameter. The location of thermocline or solar radiation effects is calibrated by changing this variable.

The code allows the user to input the frequency of output data saved. NPROF variable is used for deciding this frequency. To obtain more detailed graphs it is possible to change the NPROF values. Smaller values of NPROF means that the vertical profiles will be recorded in code with smaller time intervals.

In Chapter 4, a validation case is presented for Lake Llyn Cwellyn based on the study of Darbyshire & Edwards (1972). Their 1966 observation data was captured by the code via calibration of extinction coefficient (BETA), surface wind speed (FLUXHZ(J)) and short wave radiation (SRAD).

3.4. A Typical Case File

A typical Case file of PROBE code is explained in boxes below.

```

SUBROUTINE CASE(ICHAP)
C PROGRAM:CASE 1.1.1
C NAME: Wind Induced Water
C BY :Mehmet Yücel YETGIN
C DATE:16-11-10
INCLUDE 'PROBE:<LIBRARY>COMP86.INC'
include 'comp86.inc'
IF(ICHAP.GT.1) GOTO 10
C *****
CHAPTER 1 1 1 MODIFY DEFAULT DATA 1 1 1 1 1 1 1 1 1 1 1 1

```

C----GROUP 1.

```

TLAST=8.64E4
LSTEP=1440
TFRAC(2)=60
IGRID=1

```

<i>TLAST</i>	<i>Maximum integration time</i>
<i>LSTEP</i>	<i>Maximum number of time steps</i>
<i>IGRID</i>	<i>Index for grid</i>
<i>TFRAC (20)</i>	<i>Specification of time step</i>

C----GROUP 2.

```

ZDIM=33.
XDIM=1900.
YDIM=570.
INDARE=2
AREAHZ=1083000.

```

<i>ZDIM</i>	<i>Physical dimension in Z-direction</i>
<i>XDIM</i>	<i>Physical dimension in X-direction</i>
<i>YDIM</i>	<i>Physical dimension in Y-direction</i>
<i>INDARE</i>	<i>Index for area distribution</i>

INDARE=INDEX FOR AREA-DISTRIBUTION =1 INDICATES UNIFORM AREA =2 INDICATES LINEAR DISTRIBUTION =3 INDICATES NON-LINEAR DISTRB.,SEE MANUAL =4 DISTR. SPECIFIED IN CASE

C-----GROUP 3.

SOLVAR(1)=.TRUE.
 SOLVAR(2)=.TRUE.
 SOLVAR(3)=.TRUE.
 SOLVAR(4)=.TRUE.
 SOLVAR(5)=.TRUE.
 SOLVAR(6)=.TRUE.
 SOLVAR(7)=.TRUE.
 SOLVAR(8)=.TRUE.
 SOLVAR(9)=.TRUE.
 SOLVAR(10)=.TRUE.

1	F(I, JRHOU)=X-DIRECTION MOMENTUM
2	F(I, JRHOV)=Y-DIRECTION MOMENTUM
3	F(I, JH)=HEAT-ENERGY
4	F(I, JS)=SALINITY
5	F(I, JK)=TURBULENT KINETIC ENERGY
6	F(I, JD)=DISSIPATION OF TURBULENT KINETIC ENERGY
7	F(I, JC1)=CONCENTRATION NO.1
8	F(I, JC2)=CONCENTRATION NO.2
9	F(I, JC3)=CONCENTRATION NO.3
10	F(I, JC4)=CONCENTRATION NO.4

SOLVAR (NJM)	Selects variables to be solved for
--------------	------------------------------------

C-----GROUP 6.

ITURBM=3
 IPRSC=2

ITURBM	Index for turbulence model
IPRSC	Index for Prandtl/Schmidt number

C-----GROUP 7.

INDPX=-3
 INDPY=-3
 BETA=0.6
 PFILT=0.2
 CORI= 9.5E-5

CORI	Coriolis' parameter
INDPX	Index for pressure gradient
INDPY	Index for pressure gradient
PFILT	Pressure filtering coeff,
BETA	Extinction coefficient

$\Omega = 7.2921 \times 10^{-5}$ rad/s (e.g. for Lake Clinton)
 $f = 2 \Omega \sin(\varphi)$, φ is latitude location of Earth, (e.g. 40.13°)
 $f = 9.5 \times 10^{-5}$

C-----GROUP 8.

VST1(3)=3.35E7
 ZST1(3)=3
 ZST1(3)=4.5
 VST2(3)=5.02E7

CPHEAT of water : $C_p = 4185.5$ J/kg.K at 15°C & 101.325 Pa
 VST : Values for starting profile
 $VST1(3) = [^\circ\text{C}] \times [\rho] \times [C_p]$
 $VST1(3) = 8 \times 1000 \times 4185.5 = 3.35 \times 10^7$

C----GROUP 9.

IKBHZ (2) = 2
 FLUXHZ (2) = -0.693
 FLUXHZ(1)=-0.04
 ROULHZ=0.001
 IKBLZ(1)=1
 IKBLZ(2)=1

<i>Velocity to Flux ? = velocity x density</i>	
<i>Momentum (v1) = 2km/hr x 1.2446 kg/m³ = 0.556 m/s x 1.2466 = 0.693 kg/m²s</i>	
<i>IKBHZ(NJM)</i>	<i>Index for boundary conditions at high Z</i>
<i>IKBLZ(NJM)</i>	<i>Index for boundary conditions at low Z</i>
<i>FLUXHZ(NJM)</i>	<i>Flux at high Z</i>
<i>ROULHZ</i>	<i>Roughness length at high Z</i>

C----GROUP 11.

NSTAT=5000
 NPROF=20
 PRPROF(1)=.TRUE.
 PRPROF(2)=.TRUE.
 PRPROF(3)=.TRUE.
 DO 110 I=11,17
 PRPROF(I)=.TRUE.
 PLPROF(1)=.TRUE.
 PLPROF(2)=.TRUE.
 PLPROF(3)=.TRUE.
 RETURN

<i>NSTAT</i>	<i>Steps between station values</i>
<i>NPROF</i>	<i>Steps between profiles</i>
<i>PRPROF (20)</i>	<i>Selects printed profiles</i>
<i>PRPLOT (20)</i>	<i>Selects plotted profiles</i>

C *****

10 CONTINUE

C *****

CHAPTER 2 2 2 TRANSIENT BOUNDARY CONDITIONS, LINK TO MAIN CH.2 2 2

```

IF(ICHAP.GT.2) GOTO 20
SRAD=250.
FLXRAD=AMAX1(0.0,SRAD*PI*SIN(PI*TIME/3600./12.+1.5*PI))
QINFL(39)=1000.*SIN(2.*PI*TIME/(60.*24.*3600.))
QOUTFL(20)=1000.*SIN(2.*PI*TIME/(60.*24.*3600.))

RETURN

```

FLXRAD	Short Wave Radiation
QINFL	Inflow
QOUTFL	Outflow

C *****

20 CONTINUE

C *****

CHAPTER 3 3 3 ADDITIONAL SOURCE TERMS, LINK TO PHYS 3 3 3 3 3 3 3

```

IF(ICHAP.GT.3) GOTO 30

```

C TEXT

RETURN

C *****

30 CONTINUE

C *****

CHAPTER 4 4 4 ADDITIONAL OUTPUT, LINK TO MAIN CH.8 4 4 4 4 4 4 4

C TEXT

RETURN

C *****

END

3.5. Table of Variables Used in Cases of PROBE

In the Table 3.1, the variables used in this study in PROBE are listed. The values of these variables also given on the right hand side column. Some of these inputs are varied from case to case. For further information, one may address PROBE manual by Urban Svensson (1986). “NJM” indicates the variable solved by the code. For instance NJM=1 corresponds to x-direction velocity.

Table 3.1. Variables used in Cases of PROBE.

Group	Name	Type	Meaning	Inputs
1	N	Integer	Number of grid points	100
1	TIME	Real	Integration time	varied
1	TLAST	Real	Maximum integration time	varied
1	LSTEP	Integer	Maximum number of time steps	varied
1	IGRID	Integer	Index for grid	1
1	TFRAC (20)	Real array	Specification of time step	varied
2	ZDIM	Real	Physical dimension in Z-direction	33
2	XDIM	Real	Physical dimension in X-direction	1900
2	YDIM	Real	Physical dimension in Y-direction	570
2	INDARE	Integer	Index for area-distr.	2
2	AREAHZ	Real	Horizontal area of top cell	1083000
3	SOLVAR (NJM)	Logical array	Selects variables to be solved for	varied
6	ITURBM	Integer	Index for turbulence model	3
6	IPRSC	Integer	Index for Prandtl/Schmidt number	2
7	CORI	Real	Coriolis' parameter	varied
7	INDPX	Integer	Index for pressure gradient	3
7	INDPY	Integer	Index for pressure gradient	3
7	PFILT	Real	Pressure filtering coeff,	varied
7	QINFL(NIM)	Real array	Inflow	24
7	QOUTFL(NIM)	Real array	Outflow	24
7	PHIIN(NIM, NJM)	Real array	Properties of inflow	varied
7	FLXRAD	Real	Short wave radiation	varied, eg: 250
7	BETA	Real	Extinction coefficient	varied, eg: 0.6
8	ISTPR	Integer	Index for starting profiles	1
8	VST1 (NJM)	Real array	Value at the start of profile	varied, eg: 3.35e7
8	VST2(NJM)	Real array	Value at the end of profile	varied, eg: 6.07e7
8	ZST1 (NJM)	Real array	Depth for VST1	varied, eg: 13
8	ZST2(NJH)	Real array	Depth for VST2	varied, eg: 18
9	ITYPEH	Integer	Index for boundary at high Z	2
9	ITYPEL	Integer	Index for boundary at low Z	1
9	IKBHZ(NJM)	Integer array	Index for boundary conditions at high Z	2
9	IKBLZ(NJM)	Integer array	Index for boundary conditions at low Z	1
9	IKBOT(NJH)	Integer array	Index for behaviour at bottom	2
9	FLUXHZ(NJM)	Real array	Flux at high Z	varied, eg: 1.73
11	NSTAT	Integer	Steps between station values	5000
11	NPROF	NPROF	Steps between profiles	500
11	PRPROF (20)	logical array	Selects plotted profiles	1 to 20

Table 3.2. Options of variables used in Cases of PROBE.

IGRID=INDEX FOR GRID
IGRID=1 GIVES UNIFORM GRID
IGRID=2 GIVES EXPANDING GRID FROM LOW Z
IGRID=3 GIVES EXPANDING GRID FROM HIGH Z
IGRID=4 INDICATES THAT THE GRID IS SPECIFIED IN CASE
INDARE= INDEX FOR AREA DISTRIBUTION
INDARE=1 INDICATES UNIFORM AREA
INDARE=2 INDICATES LINEAR DISTRIBUTION
INDARE=3 INDICATES NON-LINEAR DISTRB.,SEE MANUAL
INDARE=4 DISTR. SPECIFIED IN CASE
ITURBM=INDEX FOR TURBULENCE MODEL
ITURBM=1 GIVES CONSTANT VALUE (=EMUCON)
ITURBM=2 GIVES K-E MODEL
ITURBM=3 GIVES K-E MODEL WITH BUOYANCY EFFECTS
ITURBM=4 INDICATES THAT F(I,JEMU) IS SPECIFIED IN CASE
PRSC=INDEX FOR TURBULENT PRANDTL/SCHMITH NUMBER USED FOR HEAT,SALINITY AND CONCENTRATIONS
PRSC=1 INDICATES THAT CONSTANT VALUES ARE USED.
PRSC=2 INDICATES THAT THE NUMBERS ARE AFFECTED BY BUOYANCY
INDPX=INDEX FOR PRESSURE GRADIENTS IN X-DIRECTION
INDPX=1 GIVES PRESCRIBED CONSTANT PRESSURE GRADIENTS
INDPX=2 GIVES PRESCRIBED MASSFLOW.
INDPX=3 GIVES PRESSURE GRADIENT DEVELOPMENT
INDPX=4 INDICATES THAT THE PRESSURE GRADIENTS ARE TO BE READ FROM SEPARATE FILE
ISTPR=INDEX FOR STARTING PROFILES
ISTPR=1 PROFILES ARE SPECIFIED WITH VST1(1-NJM)-ZST2(1-NJM)
ISTPR=2 PROFILES ARE SPECIFIED IN CASE WITHOUT THE USE OF VST1(1-NJM)-ZST2(1-NJM)
IKBHZ=INDEX FOR KIND OF BOUNDARY CONDITION FOR VARIABLE J AT HIGH Z BOUNDARY
IKBHZ=1 GIVES PRESCRIBED VALUE
IKBHZ=2 GIVES PRESCRIBED FLUX
IKBOT=INDEX FOR KIND OF BEHAVIOR AT BOTTOM
IKBOT=1 GIVES "CONSERVATIVE" CONDITION
IKBOT=2 GIVES "NON-CONSERVATIVE" CONDITION

The chosen options in cases of this study are highlighted with yellow colour on table 3.2. More information on other variables of the code and discretization schemes applied to the governing equations could be found in Svensson (1978) and Svensson (1986).

CHAPTER 4

RESULTS

4.1. Introduction

The aim of this chapter is to estimate and analyse the possible effect of different factors on lakes. PROBE can let us estimate these effects in a very short computational time on a common computer with a Fortran compiler. In this section, there are several scenarios and observations conducted on an artificial lake geometry.

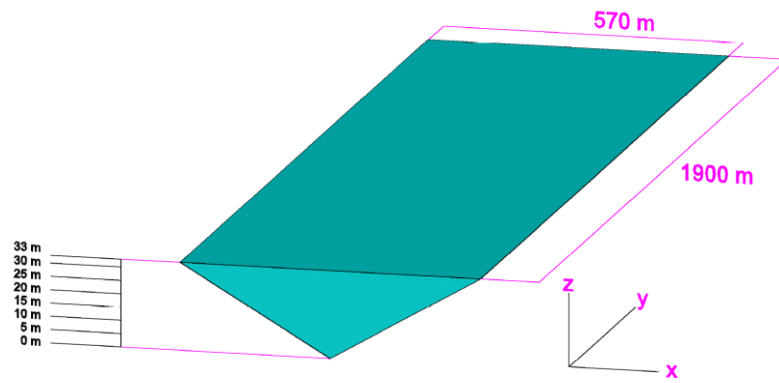
Initially, the effect of cross sectional area of the artificial lake is considered. In other words, the complex shape of the lake is simplified by assuming a rectangular and triangular lake cross section. Later, the effect of surface wind on the water column is investigated. Wind is one of the main factor which drives the mixing process in a water body. The direction of wind is considered as one of the variable in the study and its effect is discussed. Single and double direction wind is mainly considered. Furthermore, Coriolis' effect is combined with these wind effects on different cases and also different Coriolis' parameter of different latitudes are used with same initial conditions in order to isolate the effect of Coriolis over the water column in lake. A Turnover phenomenon and its simulation using the code is also discussed in this chapter.

Finally, the vertical distributions of temperature in the water column of the artificial lake under several different conditions are investigated. Temperature is affected by solar radiation directly and it influences vertical temperature distribution. By calibrating different parameters in the numerical code, measured temperature profiles are agreeably captured numerically. The inflow and outflow effects on the temperature profile in a water body are discussed. The main scenario of this study relates to an artificial lake near a nuclear power plant. It is assumed that due to this plant, hot water is released to the lake and cold water is withdrawn from it for cooling purposes of the plant. Inflow and outflow pipes at different depths are considered and changes over the thermocline are investigated. As an extra case, the effect of melted snow incoming to lake surface is also studied and effects on thermocline are observed.

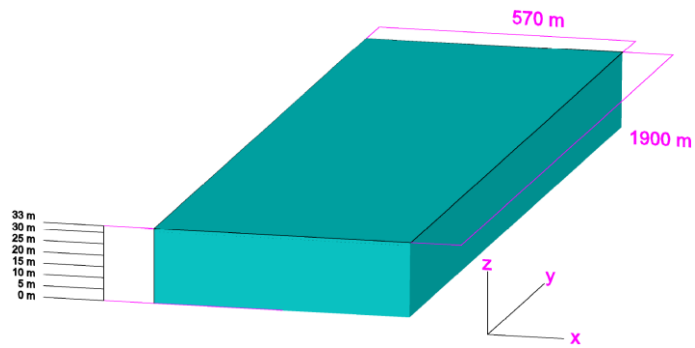
4.1.1. Simplified Shapes of Artificial Lakes

In this section, the effect of cross sectional shape of artificial lakes on vertical temperature and velocity distribution will be observed. In case file of PROBE, under Group 2, physical dimensions and area distribution index, INDARE can be given as input. INDARE=1 indicates uniform area, in other words the cross section of lake will be rectangular. INDARE=2 indicates linear distribution which provides the cross section to be triangular. To generate a parabolic cross section INDARE has to be taken as 3, furthermore variable CEXPA which stands for the expansion factor of areal distribution has to be selected. CEXPA could take values from -0.5 to 2.0. The value is typically 2.0 for Swedish Lakes (Svensson, 1986). In this study the value of CEXPA is arbitrarily taken as 0.5. This value could be evaluated based on geomorphic shape of a lake. The area of each cell AREA (I) at each grid node is calculated based on $AREA(I) = AREA_{HZ}[Z(I) - Z(N)]^{CEXPA}$. Here, Z(I) is the depth at node I and Z(N) is the depth at the final node. AREA_{HZ} represents the area of the top cell as given in Table 3.1. When INDARE=2 is selected by the user then, CEXPA is 1.0 by default.

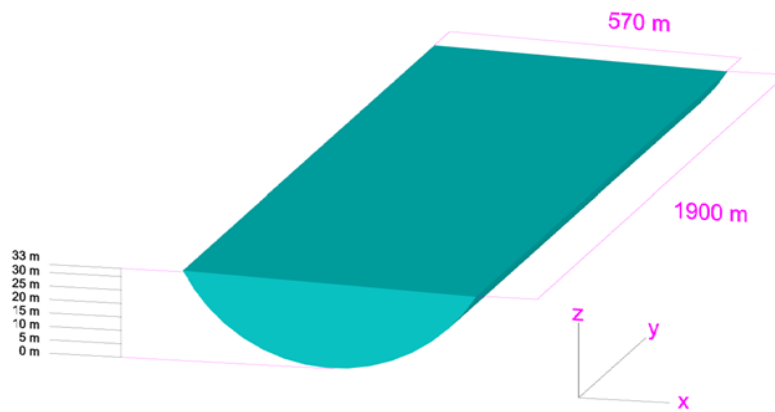
All lakes considered with different areal distributions over the vertical are assumed to have the depth of 33 m. The simplified lake geometries are given in Figure 4.1.



a)



b)



c)

Figure 4.1: Simplified shapes of artificial lake. a) triangular domain, b) rectangular domain c) parabolic domain.

The surface wind velocity is assumed as 5 km/hr and on single direction for all models. In PROBE, wind velocities have to be input as in flux forms. The unit of velocity is m/s. Velocity flux is simply the multiplication of velocity and density of air. The density of air is taken as 1.2446 kg/m³.

Velocity Flux = Velocity x Density

Momentum (v1) = 5 km/hr x 1.2446 kg/m³ = 1.39 m/s x 1.2446 kg/m³ = 1.73 kg/m²s

The temperature is taken as 8 °C at the bottom 13m of the lake and it is taken as 14.5 °C at the top 18m of the lake. These temperature values are taken from the study of Darbyshire and Edwards (1972). The thermocline in the simulations are based on 10th of August data in Figure 4.2.

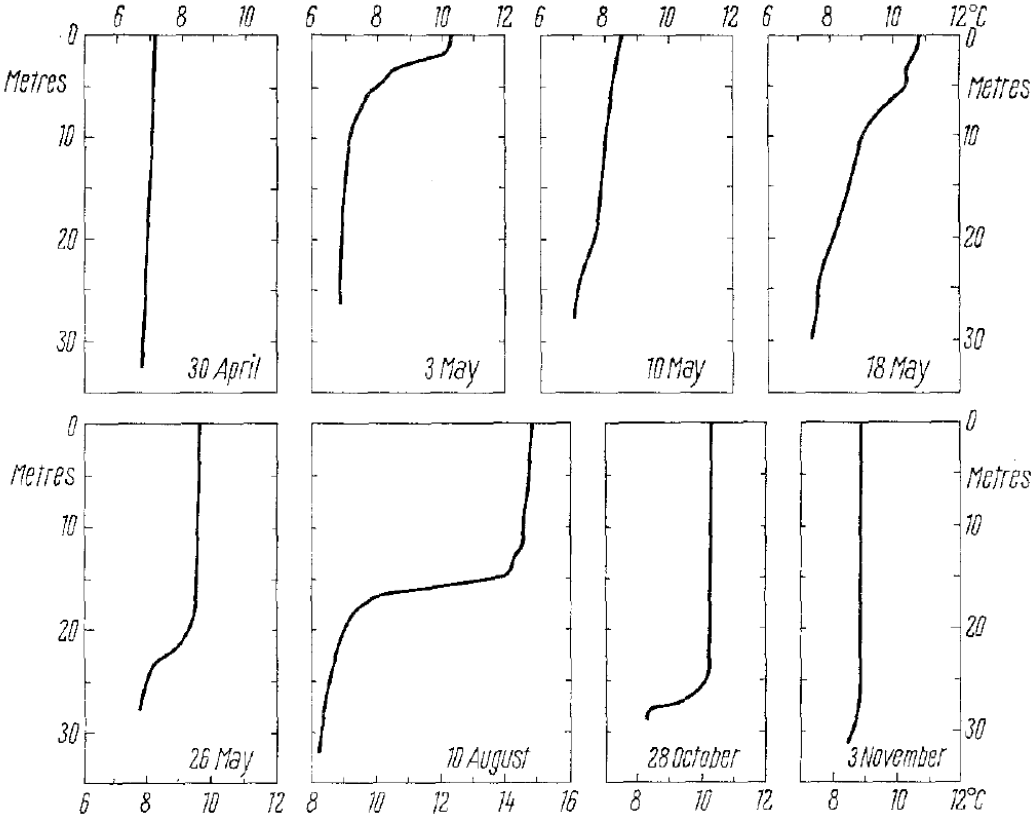


Figure 4.2: Examples of temperature profiles early and late in the season. (Darbyshire and Edwards, 1972)

Heat data needs to be entered by using heat flux over the thermocline. Specific heat capacity of the water is taken as 4185.5 J/kg°C at 15°C and atmospheric pressure is defined as 101.325 kPa by default in the code.

$$VST1(3) = [^{\circ}C] \times [\rho] \times [C_p]$$

$$VST1(3) = 8 \times 1000 \times 4185.5 = 3.35 \times 10^7 \text{ J/m}^3 \quad z=13\text{m}$$

$$VST2(3) = 14.5 \times 1000 \times 4185.5 = 6.07 \times 10^7 \text{ J/m}^3 \quad z=18\text{m}$$

If a profile for any variable needs to be imposed to the code, VST1(J) and VST2(J) variables could be used. If heat flux needs to be defined, J is taken as 3. In above equations, VST1(3) is the heat flux value defined in PROBE and “1” means the first point over the vertical where thermocline begins, which corresponds to z = 13 m from bottom of the lake. VST2(3) defines the heat flux value at the end of the thermocline where z = 18 m from bottom of the lake. The temperature output of the code is in °C. ρ is the average density of water in kg/m³ and C_p is the heat capacity of water.

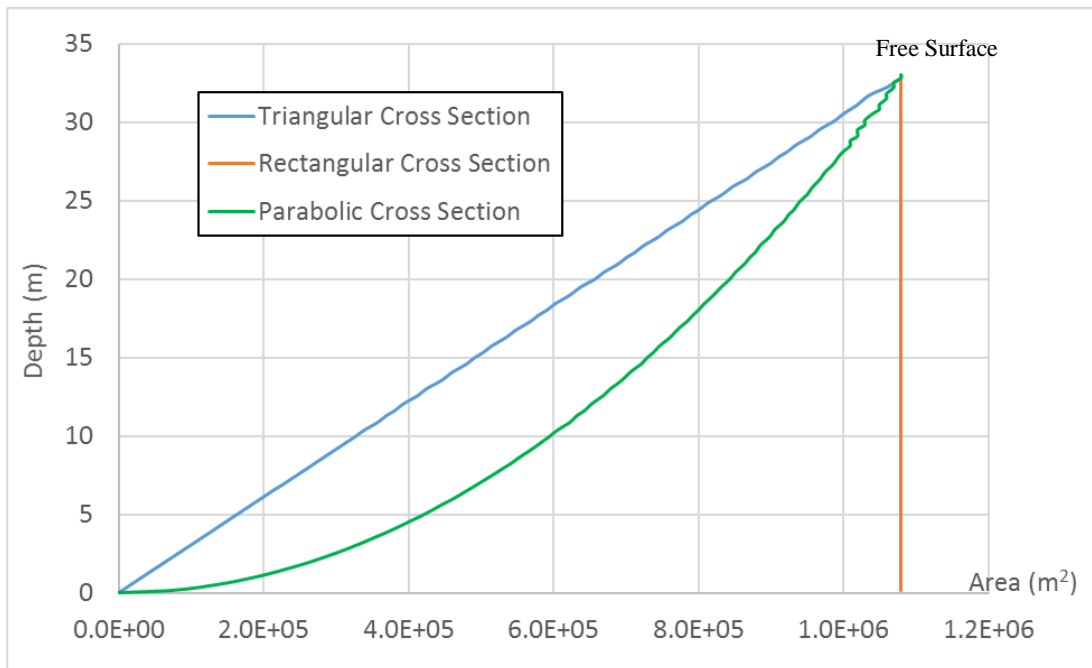


Figure 4.3: Areal distribution over the vertical for INDARE values of 1 (rectangular), 2 (triangular) and 3 (parabolic).

Figure 4.3 shows the change of surface area of the lake with respect to its depth. When code runs with the similar wind conditions and initial thermal profile for all artificial lakes considered in Figure 4.3, vertical temperature distribution in triangular shaped lake is warmer than the rectangular one. Between free surface of the lake and 5 m from the lake bottom, temperature difference is around 1°C between triangular cross-sectioned and rectangular cross-sectioned lakes. The vertical temperature distribution of parabolic cross-sectioned lake falls in between these two lakes. Figure 4.4 shows the mixing/cooling effect of wind on these lakes. The temperature differences between these three lakes simply come from volumes of the reservoir. The real bathymetry of the Lake Llyn Cwellyn is given in Figure 4.6 and it is assumed that the lake could be simplified as given in Figure 4.1a. Initial volume of warm water in a triangular lake surface is comparatively larger than the cool water volume at the bottom, where these values are comparable for rectangular and parabolic case. Triangular cross-sectioned lake represents an extreme setting.

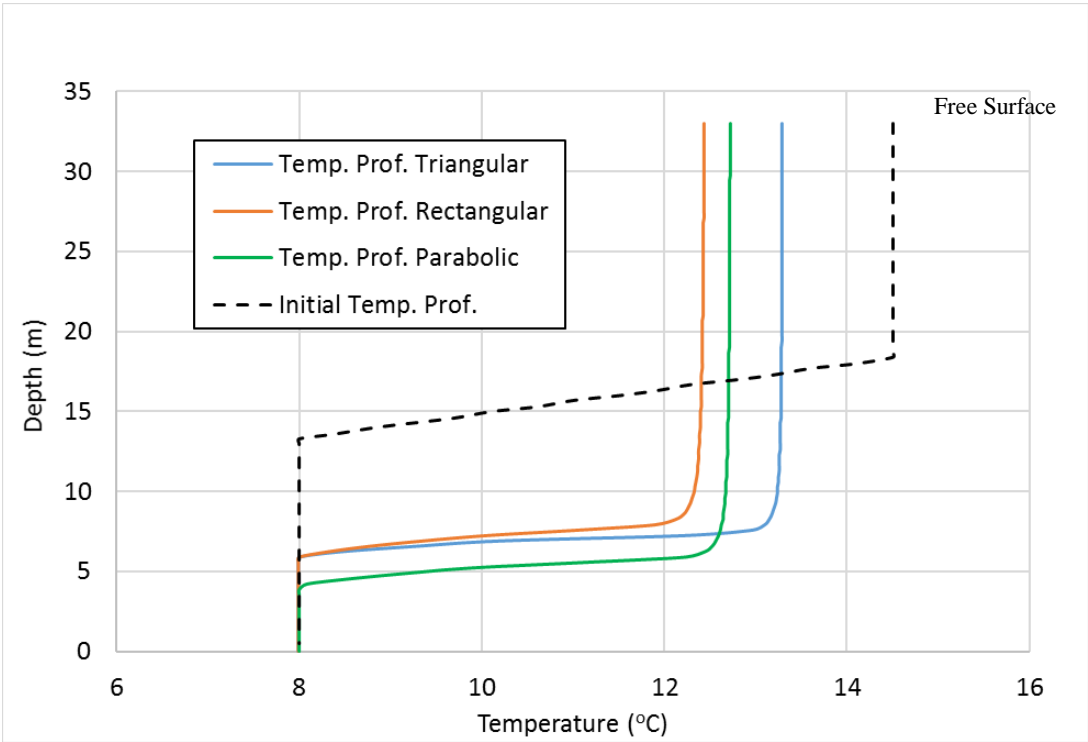


Figure 4.4: Vertical temperature distribution of models.

As seen in Figure 4.5, there are differences between three models in terms of vertical velocity distribution after the code runs for 24 hours. In parabolic lake, the velocity values are higher at deeper sections eventually reaching zero value at the bottom. This might mainly be due to enhanced wall effects imposed on a narrower horizontal plane at deeper sections in a triangular lake.

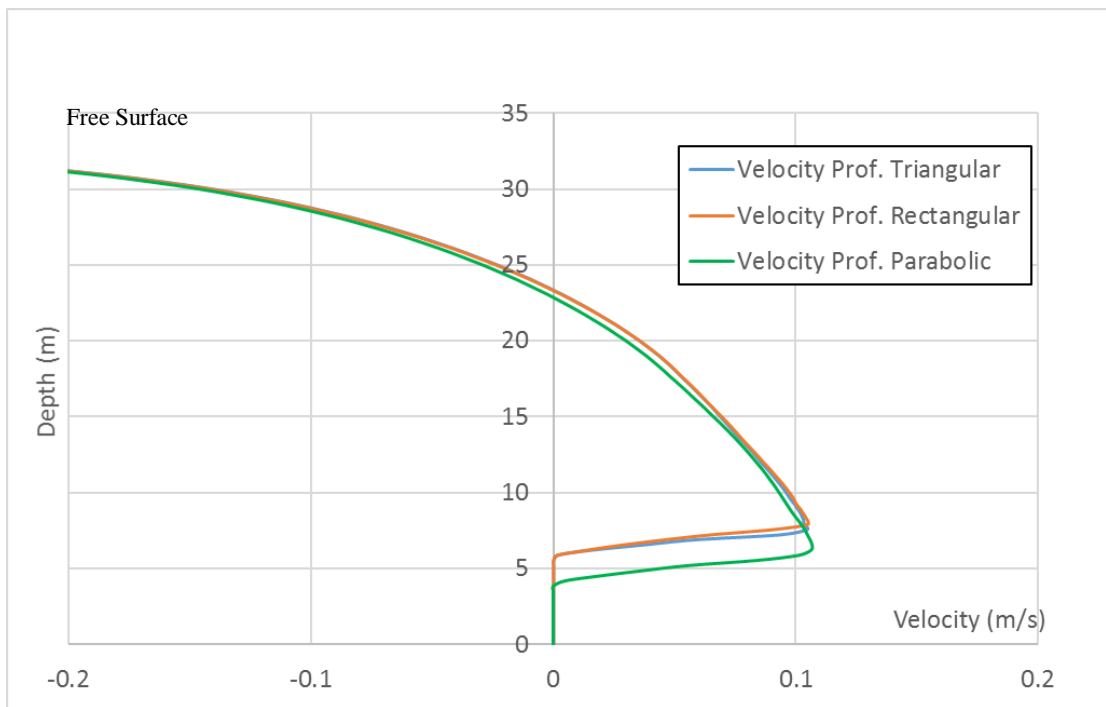
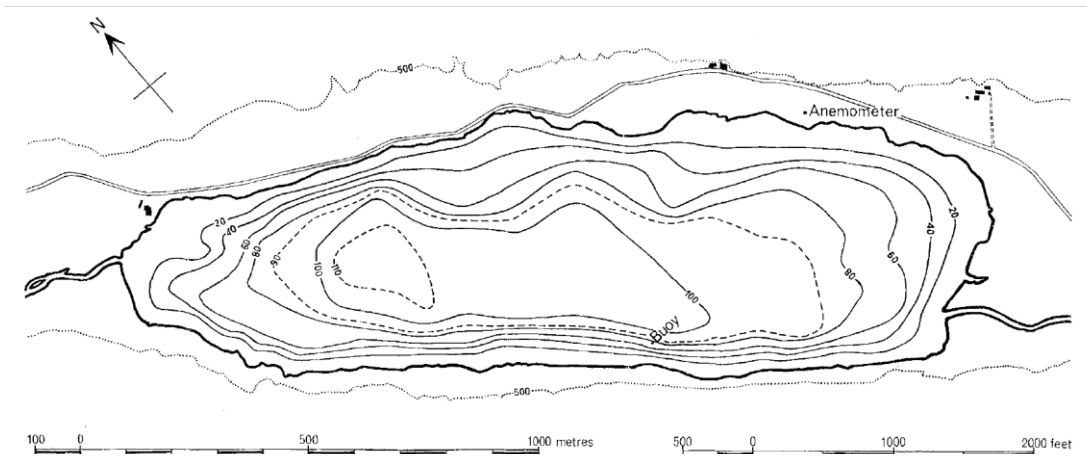


Figure 4.5: Vertical velocity distribution of models.



(a)



(b)

Figure 4.6: a) Google earth view of Llyn Cwellyn. b) Bathymetric map of Llyn Cwellyn. (Darbyshire and Edwards, 1972)

4.1.2. Wind Effects on Mixing in a Lake

Turbulent mixing in a water body usually caused by wind which is the principal source of mechanical energy to mix the water. The wind acting on the surface causes a shear force in the direction it blows (Tsanis, 1987). In spring and autumn, complete mixing of water is achieved when water within the lake is almost at the same temperature at every depth. Wind is the main driver of this process. In summer, rapid heating causes a warm water zone near the surface and wind mixes this zone so that thermocline exists near surface of the lake. In winter, if an ice cover occurs, the wind cannot mix the lake and the temperature is almost 4 °C or above at most of lake, around ice cover the temperature of water will be less than 4 °C but greater than 0 °C. The effects of wind on mixing in a lake is shown on Figure 4.7. In PROBE, time step is taken 1 minute and the total simulation is 24 hours. The wind effect shows overturn phenomena and formation of thermocline in Figure 4.7 due to seasonal effects. The driving mechanism of wind is explained in details in Limnology. (Horne and Goldman, 1994)

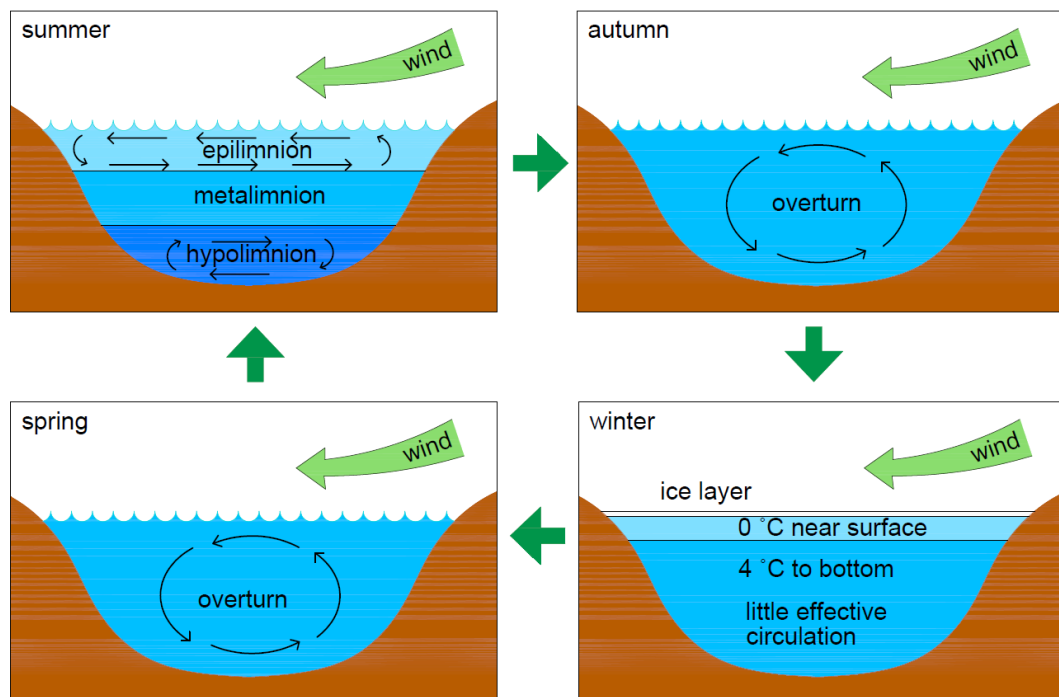


Figure 4.7: Wind effects on mixing in a lake

In this chapter wind effect is divided into two parts which are one directional and two directional winds. In two directional wind cases, the magnitude of resultant wind velocity is equal to magnitude of single directional wind cases.

4.1.2.1. Wind Velocity in Single Direction

In this section, it is assumed that the wind blows only in $-x$ direction as given in Figure 4.8.

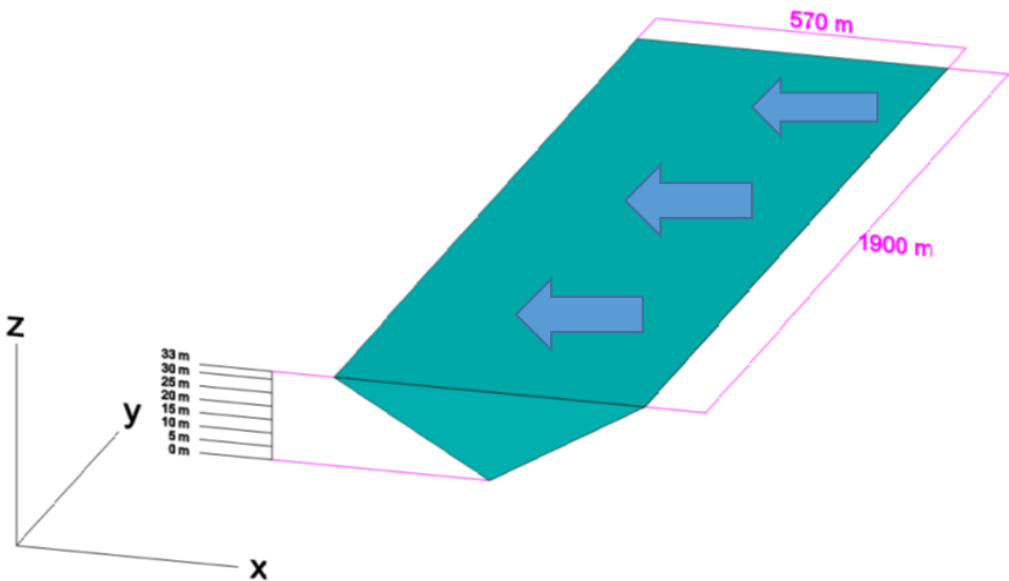


Figure 4.8: Schematic of wind blowing in single direction over a triangular cross-sectioned artificial lake.

Three different wind velocities over artificial lakes are considered. These are 5 km/hr, 10 km/hr and 25 km/hr, respectively. Based on Beaufort scale these winds can be classified as Light Breeze, Gentle Breeze and Strong Breeze, respectively. The wind speeds in Beaufort scale are based on measurements taken at a distance 10 m above the ground (Web 7). Closer to the surface the wind speed is expected to be reduced due to surface effects. Therefore, the wind speed used in this study, which represents the wind speed at the surface of the lake, is increased by 60% as suggested in the

literature and then classified using Beaufort scale (Web 7). The wind effects shall be entered in code by converting them into velocity fluxes.

$$\text{Momentum (v1)} = 5\text{km/hr} \times 1.2446 \text{ kg/m}^3 = 1.39 \text{ m/s} \times 1.2466 \text{ kg/m}^3 = 1.73 \text{ kg/m}^2\text{s}$$

$$\text{Momentum (v2)} = 10\text{km/hr} \times 1.2446 \text{ kg/m}^3 = 2.78 \text{ m/s} \times 1.2466 \text{ kg/m}^3 = 3.37 \text{ kg/m}^2\text{s}$$

$$\text{Momentum (v3)} = 25\text{km/hr} \times 1.2446 \text{ kg/m}^3 = 6.94 \text{ m/s} \times 1.2466 \text{ kg/m}^3 = 8.65\text{kg/m}^2\text{s}$$

In this representation v1, v2 and v3 means different velocities of winds, respectively. In Figure 4.9, three different magnitude single direction winds are plotted. It can be said that, when the magnitude of the wind increases, the velocity values over the column of water increases. This in return is expected to increase mixing in the lake. Wind blows in the $-x$ direction at the surface, this causes a $+x$ velocity near the lake bottom as can be seen in the figure. This causes a counter clockwise cycle in the water body. UVEL in the figure indicates the velocity in the x-direction.

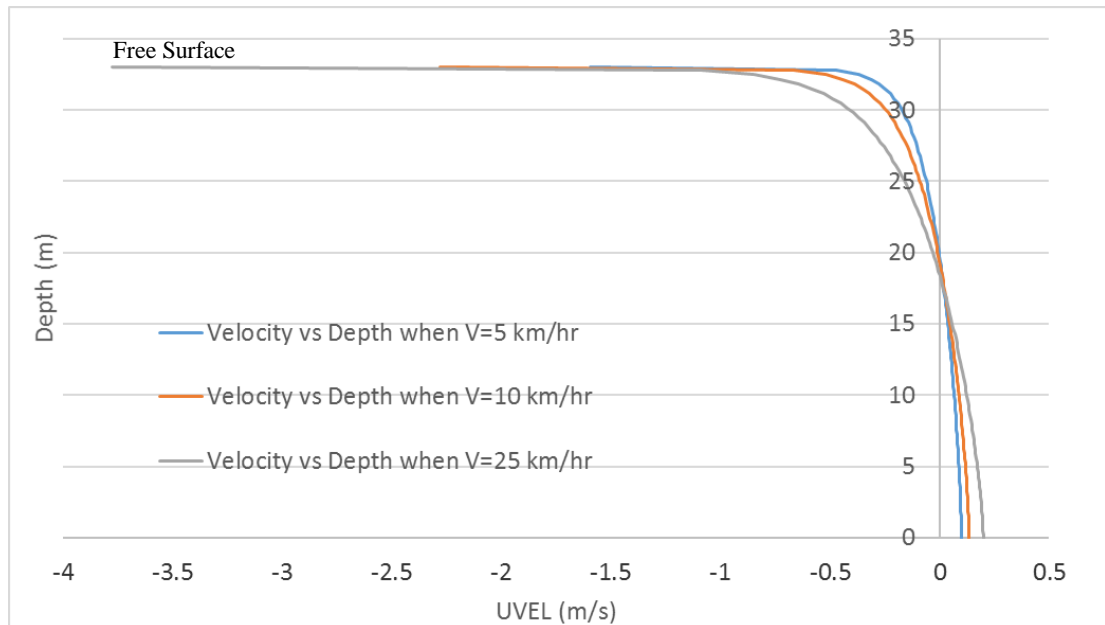


Figure 4.9: Velocity profiles of three different magnitude single direction wind

4.1.2.2. Wind Velocity in Two Directions

In this section, it is assumed that the wind blows both in -x and y directions as given in Figure 4.10.

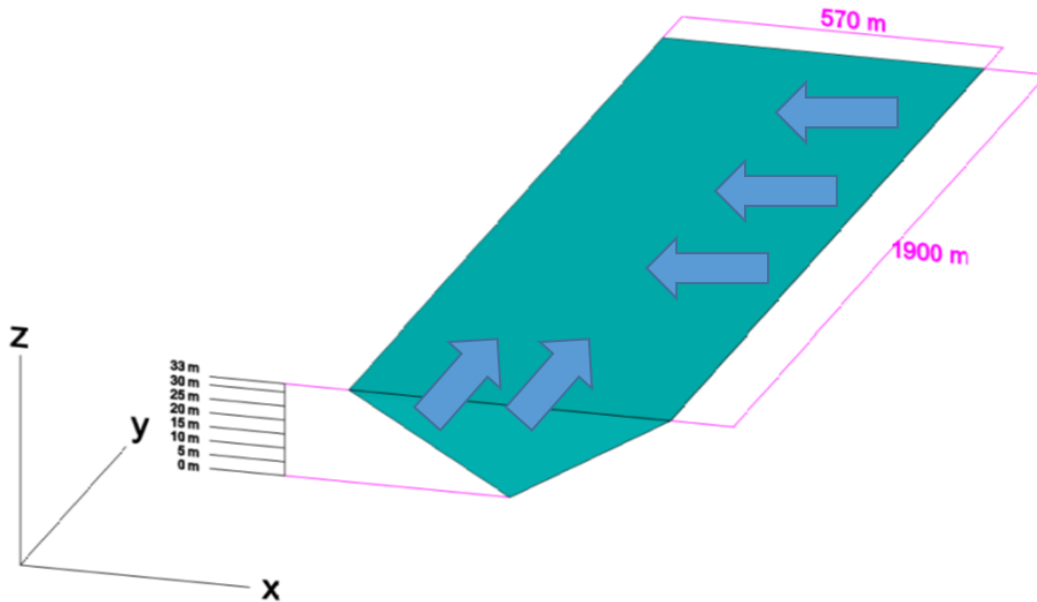


Figure 4.10: Schematic drawing of wind on two directions

The resultant forces are equal to the magnitudes considered in single direction cases (5, 10, and 25 km/hr) and shown in Figure 4.11. Third case considered shows the unsymmetrical division of velocity components of 10 km/hr velocity wind.

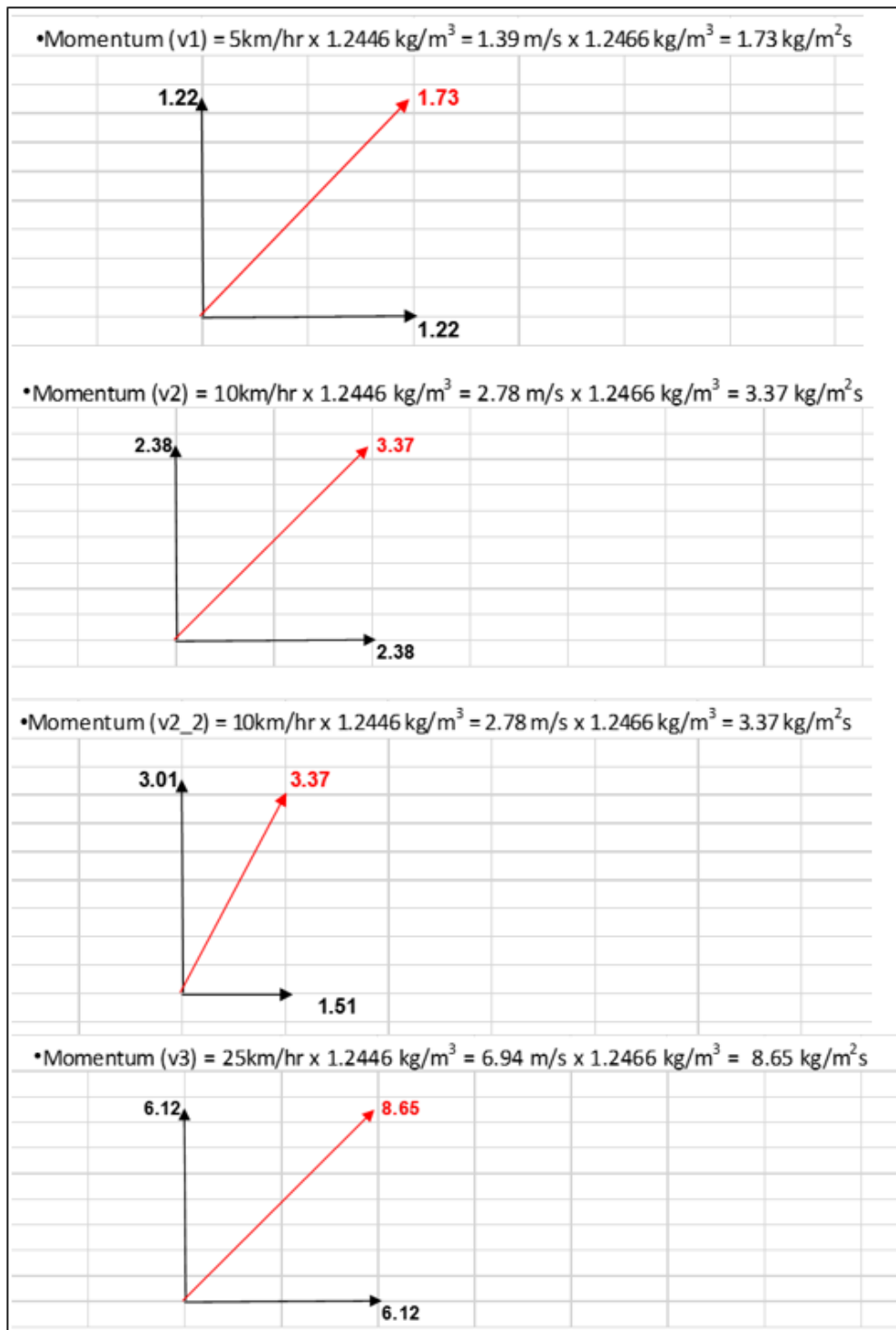


Figure 4.11: Divided fluxes into two directions without changing magnitude of the resultant.

In Figure 4.12, vertical velocity profiles within the lake due to $V=5$ km/hr single direction wind is compare to the one due to two direction. But, when the magnitude divided into two parts, the velocity on the x direction became slower and velocity value on the surface and on the bottom of the lake in x-direction became smaller. However, two directional wind introduces velocities in y-direction within the water column of the lake, VVEL, as seen in Figure 4.12. Previously mentioned counter rotating cycle forms in both directions and the mixing process becomes more complex within the lake. This shows the crucial effect of wind direction over the lake.

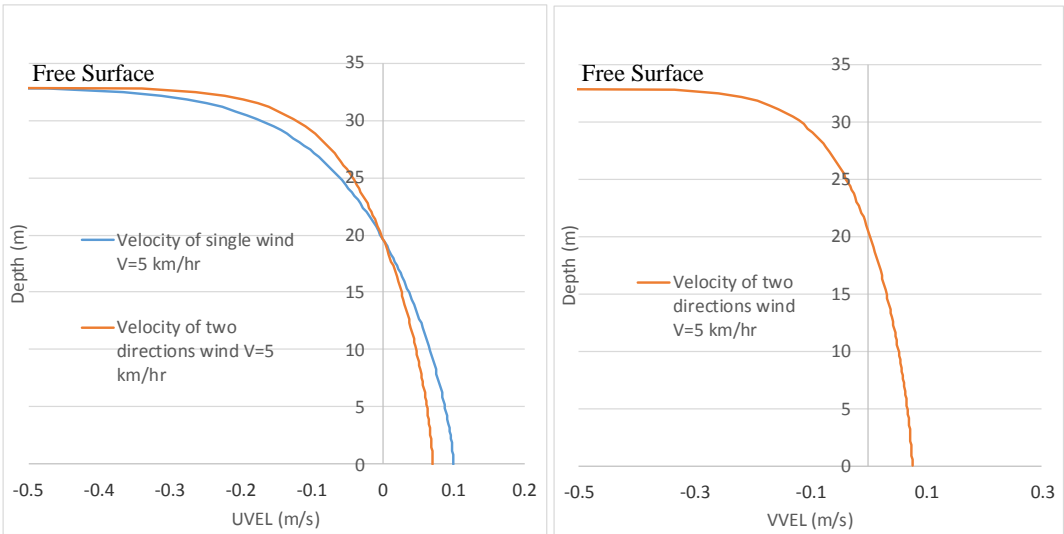


Figure 4.12: Velocity profiles of (x direction) single and two direction winds

In Figure 4.13, the velocity profiles that belongs to v_2 & v_{2_2} of Figure 4.11 are given. When observing same resultant magnitude with different directional winds, the direction of observation is important. The y-direction wind is considered in the figure. The flux on y direction of v_2 is $2.38 \text{ km/m}^2\text{s}$ and for v_{2_2} is $3.01 \text{ km/m}^2\text{s}$, with this minor change in the wind flux at the surface it was still possible to observe a change in vertical velocity distribution in a 33m-deep lake as given in Figure 4.13.

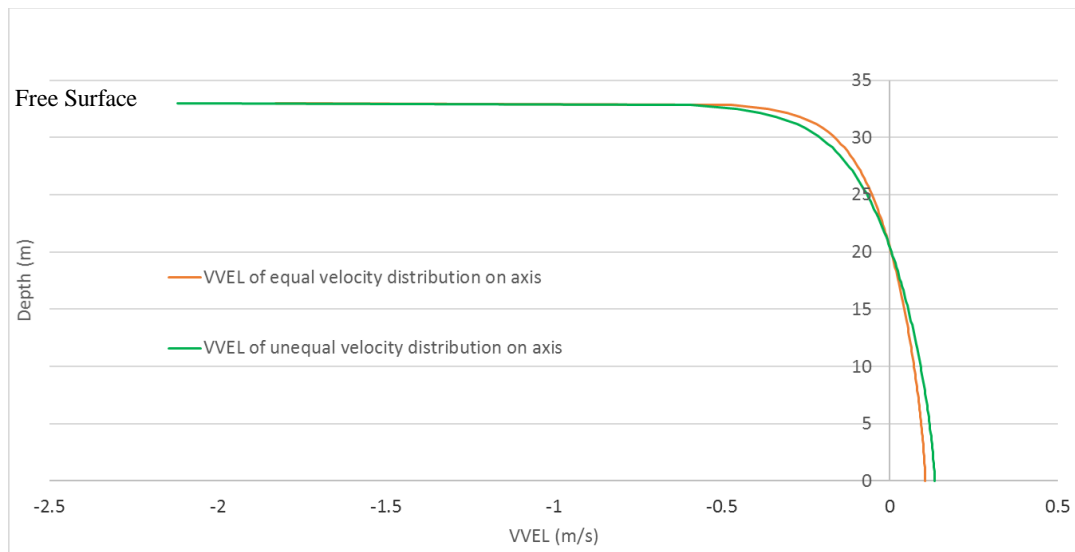
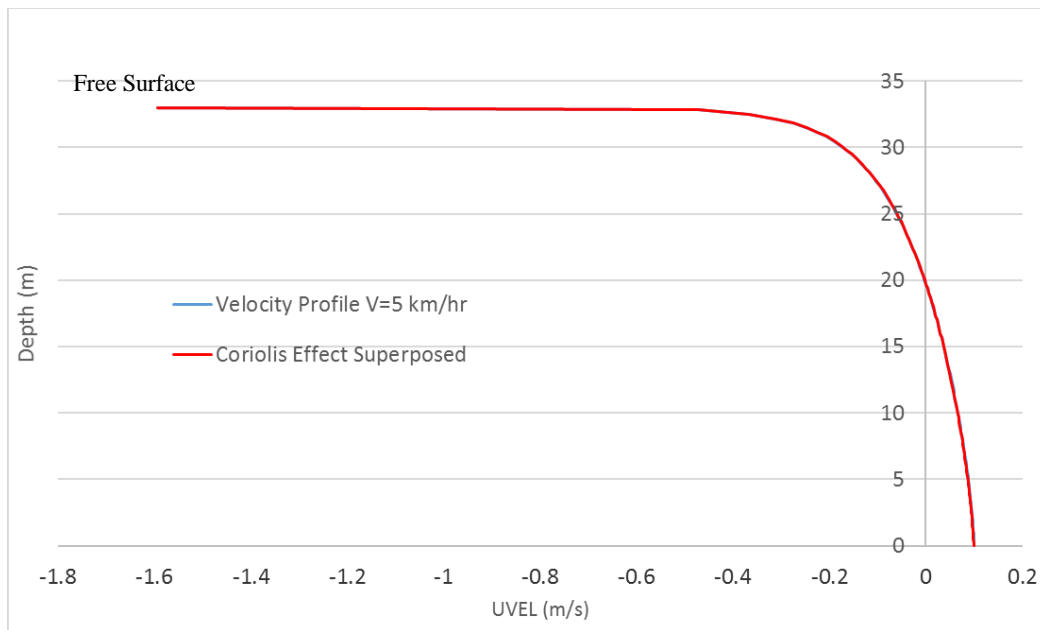


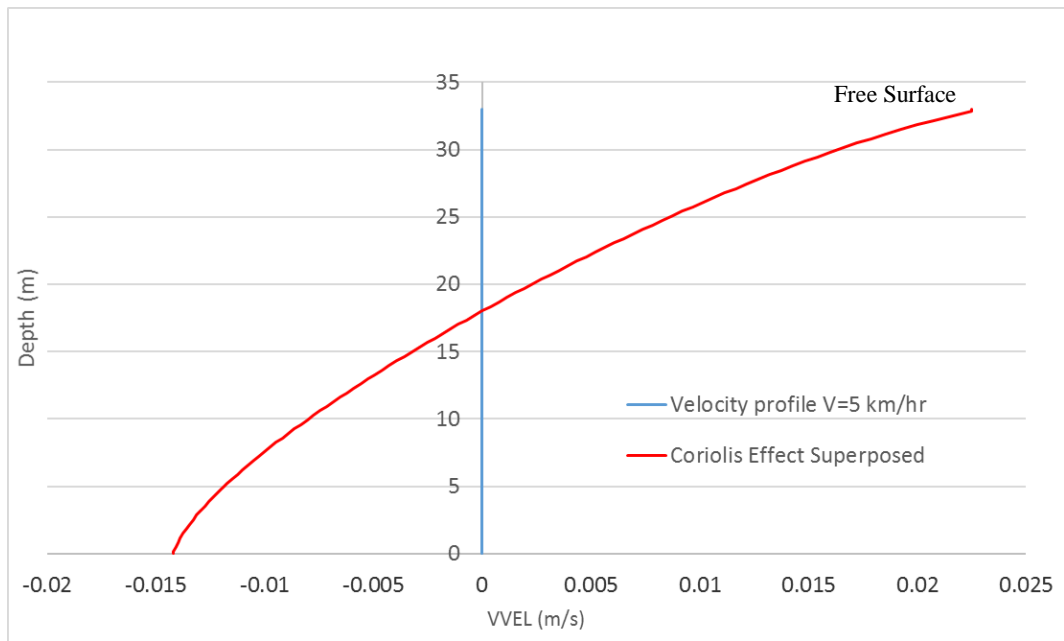
Figure 4.13: Vertical velocity profiles in the lake due to same magnitude wind with different velocity components, equal (v2) and unequal (v2_2) distribution on x and y directions.

4.1.3. Coriolis' Effect Combined with Wind Effect

Due to world's rotational motion there exists Coriolis' effect. This effect deflects the winds. Normally, winds transfer from high-pressure to low pressure system and do not blow on a straight line. The real route of winds and oceans are partly result of Coriolis' effect. In this subsection, the same wind effect in the previous section are superposed with Coriolis' effect measured on Lake Llyn Cwellyn and the results are plotted. The wind speed is taken as 5 km/hr solely in x-direction, the Coriolis' effect with value of $9.5e-5$ rad/s is superimposed. It is seen from the Figure 4.14a that there are no differences. This is because of the single direction wind effect which could be explained by equations (2 and 3) in Chapter 3. In governing equations Coriolis' effect is given by f parameter, which appears to couple with cross direction velocities. Therefore we cannot observe with u-direction wind any effect of Coriolis. However, as indicated in Figure 4.14b Coriolis' effect can be observed in the VVEL. Although the VVEL magnitude is zero when Coriolis is neglected, there exists a velocity profile when Coriolis is considered.



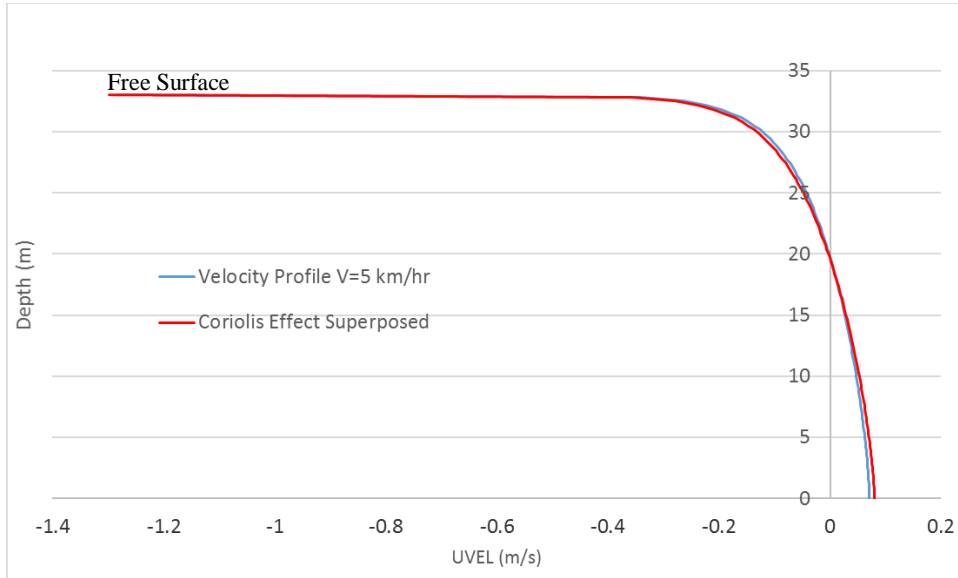
(a)



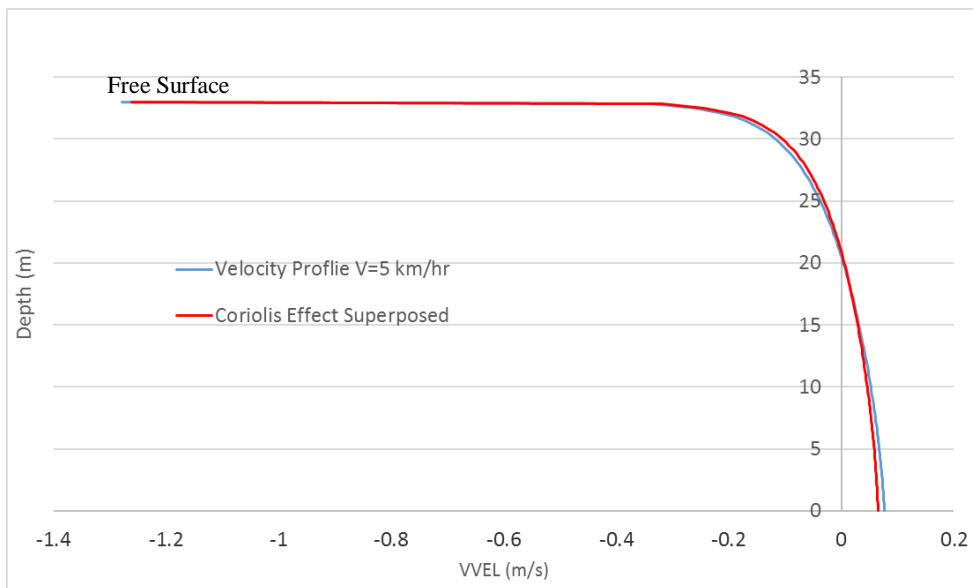
(b)

Figure 4.14: The graph of single direction wind (5 km/hr) and Coriolis combined situation: a) U-velocity b) V-Velocity

If double direction wind is taken into account effect of Coriolis is on both directions as seen in Figure 4.15.



(a)



(b)

Figure 4.15: Vertical velocity distribution over the water column due to combined effect of two directional wind and Coriolis' effect: a) U-velocity b) V-Velocity

If two directional wind case is considered, the effect of Coriolis is on both directions. Therefore, this effect is as not pronounced as in Figure 4.14b.

To search the effect of different Coriolis' parameters with same initial conditions, three different locations are taken randomly as given in Figure 4.16. By using two directional wind speed with resultant force 5 km/hr these three f values and its effects are analysed. Coriolis' effect can be calculated as:

$f = 2 \Omega \sin (\phi)$, where ϕ is the latitude of the locations, Ω is $2\pi/(24 \text{ hours})$ the angular velocity of the world around its axis (Web6).



Figure 4.16: Coriolis parameters of different locations on earth. (Image is from Google Earth.)

Due to these explanations, Coriolis' parameters of selected cities are given below;

$$f_{\text{Stockholm}} = 1.251 \times 10^{-4} \text{ rad/s} \quad (\text{Latitude / Longitude : } 59^{\circ} 20' 05'' \text{ N / } 18^{\circ} 03' 48'' \text{ E})$$

$$f_{\text{Mersin}} = 0.871 \times 10^{-4} \text{ rad/s} \quad (\text{Latitude / Longitude : } 36^{\circ} 48' 44'' \text{ N / } 36^{\circ} 38' 29'' \text{ E})$$

$$f_{\text{Kuala Lumpur}} = 0.8 \times 10^{-5} \text{ rad/s} \quad (\text{Latitude / Longitude : } 03^{\circ} 11' 14'' \text{ N / } 101^{\circ} 42' 13'' \text{ E})$$

The outputs are shown in Figure 4.17. According to these results, as approaching the poles, Coriolis' effect increases. Therefore, under the same conditions, the biggest velocity at the bottom belongs to Stockholm and the smallest belongs to Kuala Lumpur. Mersin has a mid-value.

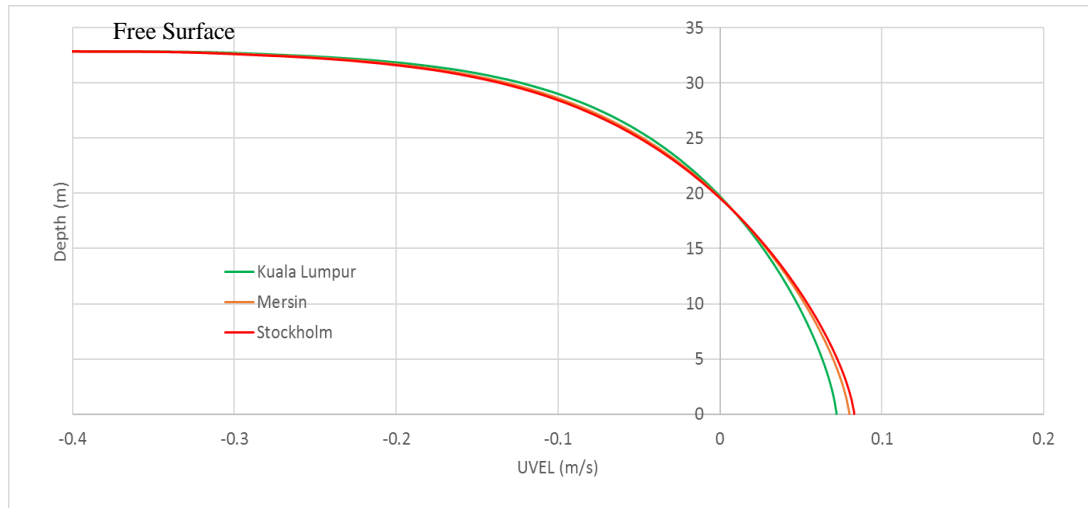


Figure 4.17: Velocity profiles under same conditions for different latitudes, hence different f values.

4.1.4. Turnover Phenomenon

Especially in autumn, when the vertical temperature distribution of lakes is observed, it can be said that the water is warmer at the bottom and cooler near the surface. This causes an unstable stratification inside the lake. Because of the fact that density of cool water is greater than warm water, the cool water tends to sink. With the effect of surface wind taken as little as 0.03 km/hr in this study, the lake starts mixing. This mixing process is referred as “turnover”. Mixing of warm and cool water takes as little as 8 minutes, however, it still depends on volume of the lake considered. After turnover the temperature profile becomes uniform over the whole water body. The phenomenon is quite unstable and causes rapid change in velocities within the lake, has turbulent characteristics, therefore, in the simulation of this phenomenon time step is taken smaller than the previous cases. Time required to obtain a fully mixed 33m-deep lake

is about 8 minutes, however it should be noted that any solar radiation effect is neglected in this case. Time step is taken 0.01 second to stabilize the code in the case of an unstable stratification. In this section, it is assumed that, the temperature at $z=28\text{m}$ depth from surface is 14.5°C and the temperature at $z=13\text{m}$ depth from surface is 8°C . The heat fluxes are calculated as below;

$$\text{VST1}(3) = [^\circ\text{C}] \times [\rho] \times [C_p]$$

$$\text{VST1}(3) = 8 \times 1000 \times 4185.5 = 3.35 \times 10^7 \text{ J/m}^3 \quad z=13 \text{ m}$$

$$\text{VST1}(3) = 14.5 \times 1000 \times 4185.5 = 6.07 \times 10^7 \text{ J/m}^3 \quad z=28 \text{ m}$$

It can be seen from Figure 4.18 that, at the beginning of process, there is an unstable stratification in the lake which is warmer at the bottom and cooler at the surface. The mixing in the lake is reported at $t=5\text{min}$ and $t=8\text{min}$. At the end of the process the lake is mixed completely and almost every point the temperature value is equal to 12.03°C .

It should also be noted that surface wind might cause the process to take even shorter amount of time.

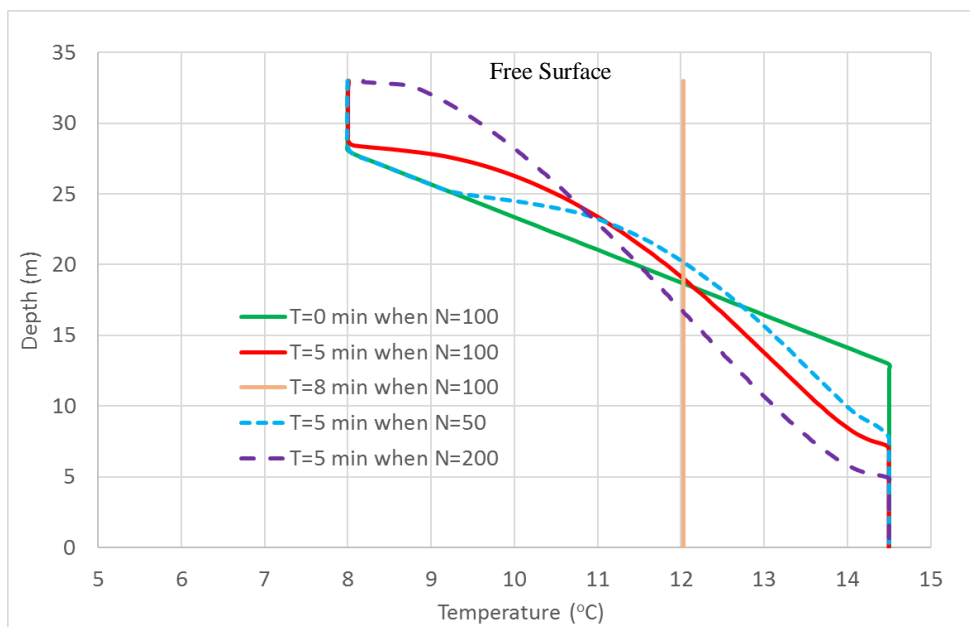


Figure 4.18: Vertical Temperature Distribution during Turnover

The other observation is about number of points used in PROBE, in other words by choosing $N=50$, the depth of the lake is divided into 50 pieces and by choosing it 100, it is divided into 100 pieces, and at $N=200$ the depth is divided into the 200 parts. As illustrated in Figure 4.18, when $N=200$ the curve became smoother at $t=5\text{min}$. But, the end result remains unchanged. Total time required to reach fully mixed conditions is 8 minutes for all N values considered. Changing number of points over the depth in complex turbulent cases might affect the profiles observed in time. Sensitivity analysis might be considered when determining the number of nodes needed for the problem at hand.

4.2. Effect of Solar Radiation - Validation of the Code

In order to validate the code capabilities on thermocline development, field study of Darbyshire and Edwards (1972) was taken as benchmark. Their work describes the formation of a thermocline in Lake Llyn Cwellyn in North Wales in summer months. The field measurements in the lake were taken from May to November in 1966. In their study it is mentioned that the wind speed and daily air temperature for Valley were taken from Air Ministry Daily Weather Report of 1966, unfortunately, this report could not be retrieved. However, Meteorological Office of UK offers monthly average values of highest and lowest temperatures for Valley together with average sun hours of that month for the year 1966. The historic values are given in Table 1. Sun hours represents the hours that sun was observed in that month. Based on these values, the code is calibrated in terms of shortwave radiation and wind speed. The initial temperature profile in the lake measured in 30th of April is given as an input to the code. The initial profile can be seen in Figure 4.19. The code also requires an extinction coefficient for the lake. This is due to the fact that only certain fraction of the incoming short wave radiation is assumed to be absorbed at the surface; this value is taken to be 0.4 as the default/recommended value in the code. The extinction coefficient (β) defines the decay of shortwave radiation as one goes deeper in the lake. The value of the coefficient for this lake is taken as 0.14. The short wave radiation is assumed to

follow a sinusoidal trend in the day time with maximum values at noon and minimum values at early and late hours of the day. The change of short wave radiation is given in Figure 4.20. The time step is taken as 10s in the code for the validation cases. Two separate runs were conducted. The short-term run is to capture the change in temperature profile in first three days of May in 1966. The long-term run is to capture the temperature profile observed in August 10th in 1966.

Table 4.1. Historic temperature, rain and sun hour data for Valley, North Wales (Web 5)

YEAR	MONTH	MAX T (°C)	MIN T (°C)	Rain (mm)	Sun Hours (hr)
1966	5	14.2	7.8	54.5	259.9
1966	6	17.1	11.8	81.1	175.8
1966	7	17.8	11.8	47.3	210.8
1966	8	18.1	11.4	88.4	189.4
1966	9	17.4	10.9	76.3	153.4
1966	10	13.7	8.3	98	106.9

In the first simulation, code runs for the three-day duration with the wind speed, extinction coefficient and shortwave radiation values calibrated. In Figure 4.21, temperature profile of the lake for 3rd of May, 1966, obtained through numerical simulation is compared to the measured one. In the first three days of May in 1966 no strong wind effect is considered only a small disturbance of 0.002 m/s surface flux is given as input in order to activate the momentum equations of the code. SRAD value is taken as 210 W/m². These values could be assumed to represent a warm spring time with no-wind condition. As can be seen from Figure 4.21, with the calibrated values of SRAD, β and wind speed, the code is capable to produce the measured field results. In this figure it can be observed that with a small disturbance at the free surface and surface heating, a thermocline starts to form with high water temperature values in the

first few meters below the lake free surface. Even though the starting profile represents a close-to-well-mixed temperature condition in the lake, the temperature within a 33 m-deep lake could change quite significantly in three-day duration.

In this regard, if the outside conditions are properly measured around a lake area, the temperature variations within the lake and possible outcomes of temperature changes in the lake could be estimated using this 1D code. Depending on the detail of the input available one can capture the day-to-day change in temperature profile in the lake.

Unfortunately, daily variation of wind and solar radiation were not available for this lake for the year 1966, therefore, a long-term analysis is carried out to investigate if the observed thermocline in 10th of August could be captured by assuming an average wind speed and average short wave radiation value for the duration between 30th of April and 10th of August, 1966. The initial temperature profile in this long-term run is unchanged and taken as in Figure 4.19. Starting with this profile code runs for about a hundred-day period. SRAD is taken as an average value of 45 W/m². At the surface both in x and y directions a surface flux with an average speed of 0.012 m/s is applied. Extinction coefficient is also kept unchanged at 0.14. Figure 4.22 shows that the general trend of the thermocline observed in August is captured via numerical model. Simulation results show that using a long-term averaged value of wind speed and SRAD, one can capture the temperature profile of 10th of August in a 100-day long simulation. However, in order to capture any variation of temperature accurately for a certain date in between end of April and 10th of August, the detailed variation of wind and solar radiation should be fed to the code.

In the validation runs effect of Coriolis is also taken into account. Based on the latitude that the Lake is located, f value is taken as 1.221×10^{-4} rad/s.

Short-term validation case which looks into the change in temperature profile in a duration of three-days, takes about 7 minutes to run on a simple laptop computer, while the long-term validation case that covers a period of hundred-days takes about 25 minutes on the same computer. In these simulations, number of nodes over the vertical

is taken as 100 and the results are observed to match satisfactorily. Therefore N is taken as 100 in all the other applications reported in the coming subsections.

This validation shows the applicability of the 1D method for fast estimation of temperature changes in water bodies under different scenarios. This is especially important in operation of power plants that uses an artificial lake as the cooling water source. In following subsections, different scenarios are considered for a lake of similar size of Lake Llyn Cwellyn, which is assumed to be used by a power plant that uses the lake as a cooling water source.

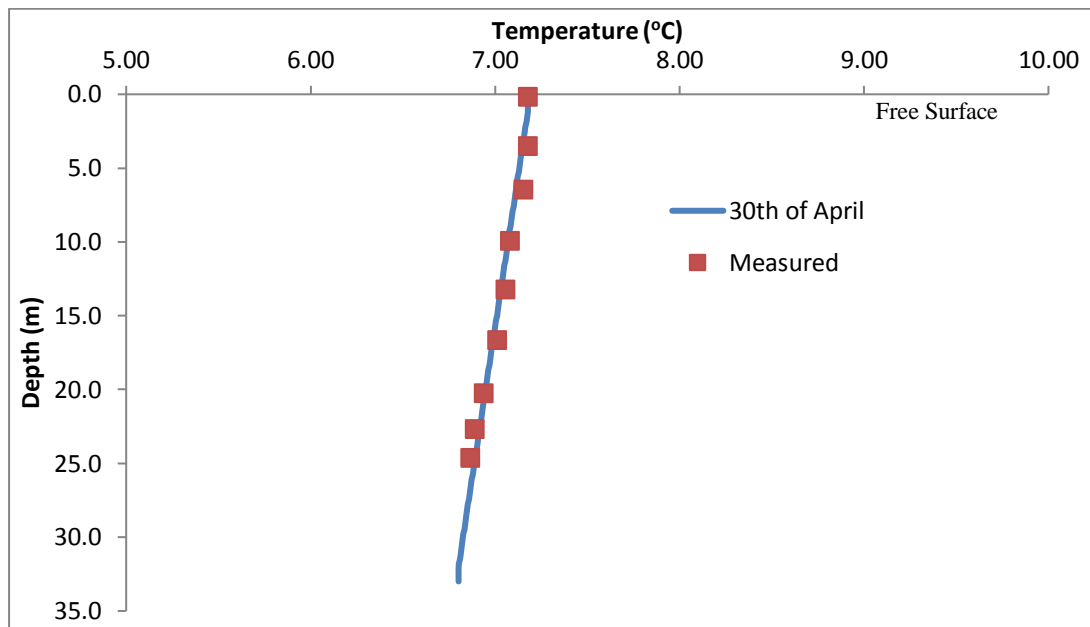


Figure 4.19: Initial profile of temperature within Lake Llyn Cwellyn measured on 30th of April, 1966. Red squares represent the field measurements, blue line is the profile given as input to the code.

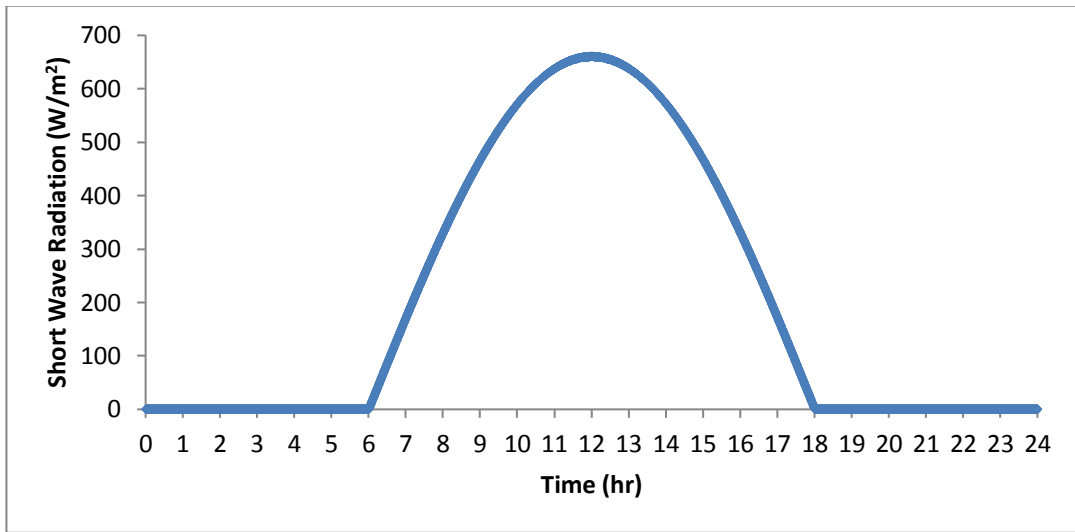


Figure 4.20: An example of sinusoidal variation of short wave radiation in 24 hours given as an input in the code.

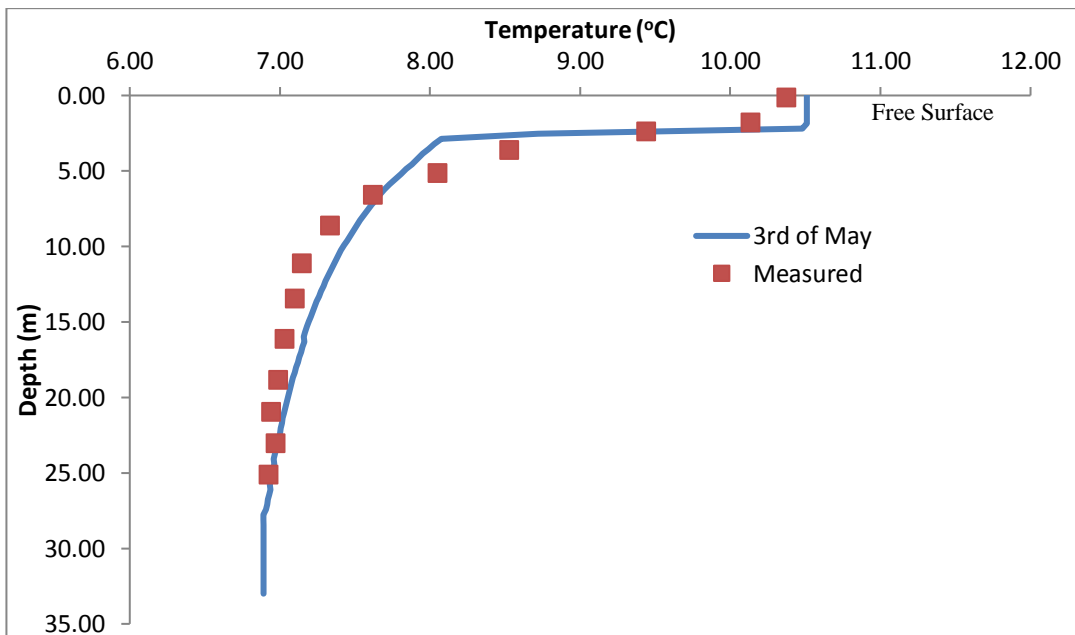


Figure 4.21: Numerical result (blue line) is compared to the measured field profile of temperature (red squares) in the lake on 3rd of May, 1966. The initial condition for the run is given in Figure 4.19.

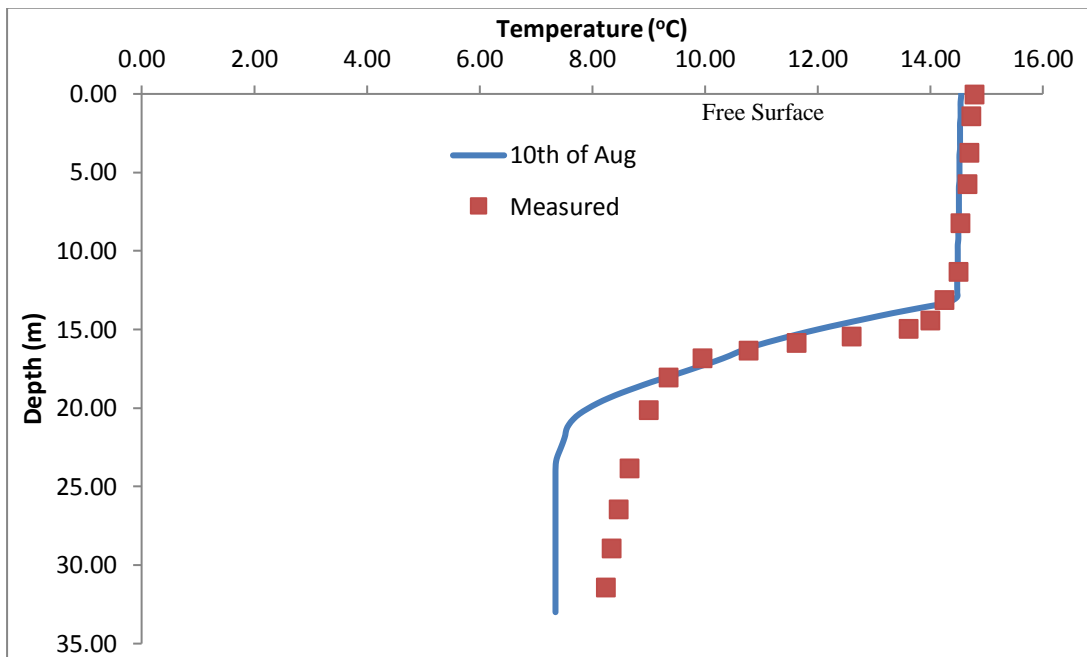


Figure 4.22: Numerical result (blue line) is compared to the measured field profile of temperature (red squares) in the lake on 10th of August, 1966. The initial condition for the run is given in Figure 4.19.

4.3. Inflow and Outflow Effects

4.3.1. Effect of Location of Outflow and Inflow

This section focuses on release of high temperature water to still water bodies such as lakes and reservoirs. The effect of high temperature water release and low temperature water withdrawn from the lake in mixture processes will be investigated numerically using different cases that are relevant to such events observed in man-made scenarios for instance, during the cooling operations of nuclear power plants.

In this section, the locations of the inflow and outflow are the variables. The thermocline of 10th August on Figure 4.1 is used as the initial temperature distribution. Inflow and Outflow at three different locations are considered. According to Water

Pollution Control Regulations (Su Kirliliği Kontrol Yönetmeliği – SKKY, 2004) of Republic of Turkey provided by Ministry of Environment and Forestry, the temperature of the discharged water, should not exceed 35 °C. Therefore, it is assumed that the outflow heat flux is equal to below if 33 °C;

$$\text{Heat Flux} = [\text{°C}] \times [\rho] \times [C_p]$$

$$\text{Heat Flux} = 33 \times 1000 \times 4185.5 = 1.38 \times 10^8 \text{ J/m}^3$$

Furthermore, based on Water Pollution Control Regulations (2004), the discharge of cooling water from a mid-size nuclear reactor is 86 m³/h which is equal to 24 m³/s. This is taken as input of PROBE as QINFL and QOUTFL under Group 6 in the CASE file. QINFL and QOUTFL are taken as identical in order to avoid any change in water depth in the lake.

In case 1, hot water is released to the reservoir at almost free surface and the outflow is at the bottom of the reservoir. In case 2, both inflow and outflow are located at the mid-depth of the reservoir at the centre of the thermocline. In last case, the inflow is at the mid-depth and the outflow is taken at the bottom. The simulation time is 24 hours and the heating effect from solar radiation is neglected to see the effect purely of inflow and outflow. Time step of the simulations is taken as 1 minute.

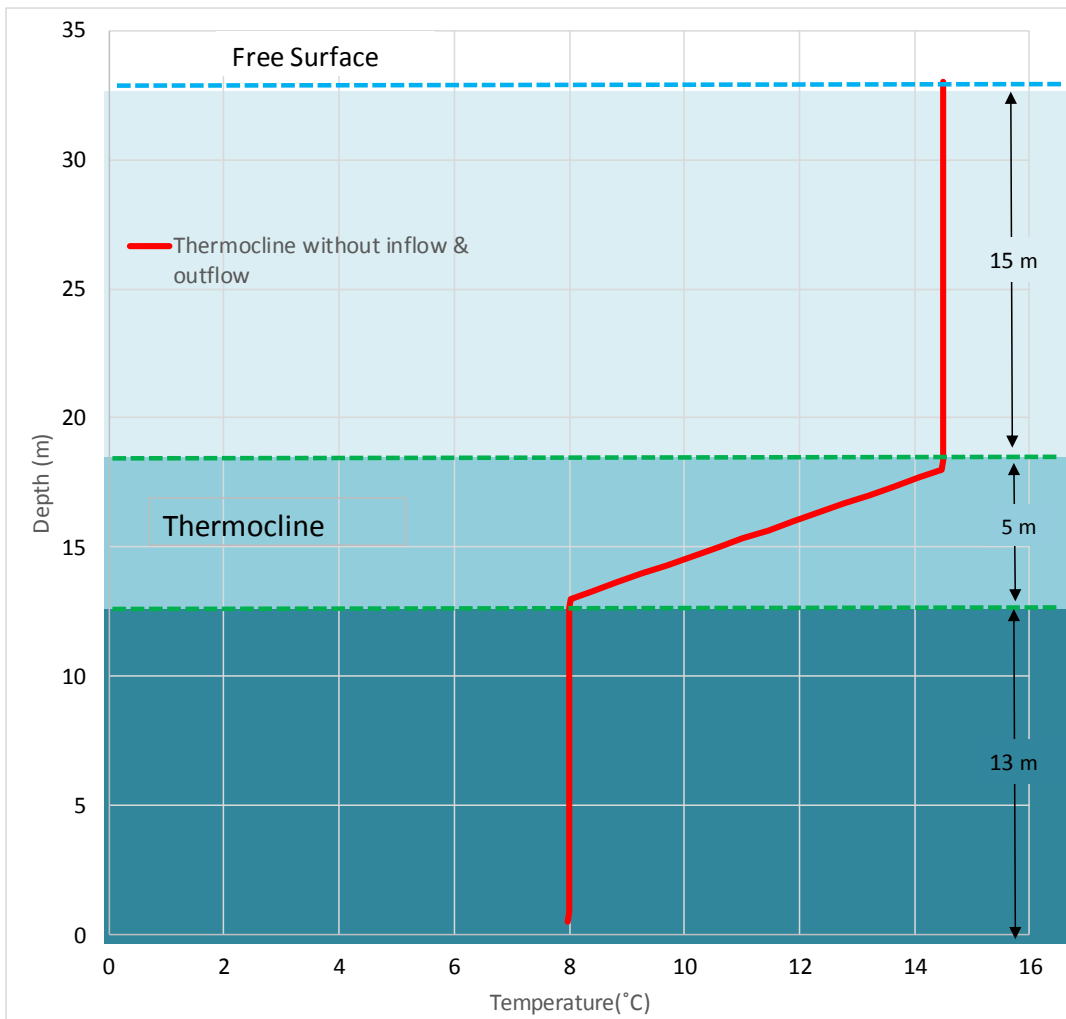


Figure 4.23: Initial temperature distribution without inflow & outflow.

Without any inflow and outflow, the vertical temperature distribution of the lake is given in Figure 4.23. The zone of 15m from the surface is epilimnion zone of the lake. The middle zone which is about 5 m is the Thermocline in other words metalimnion. This zone has the optimum conditions for habitats. The deepest zone of 13m is called hypolimnion zone.

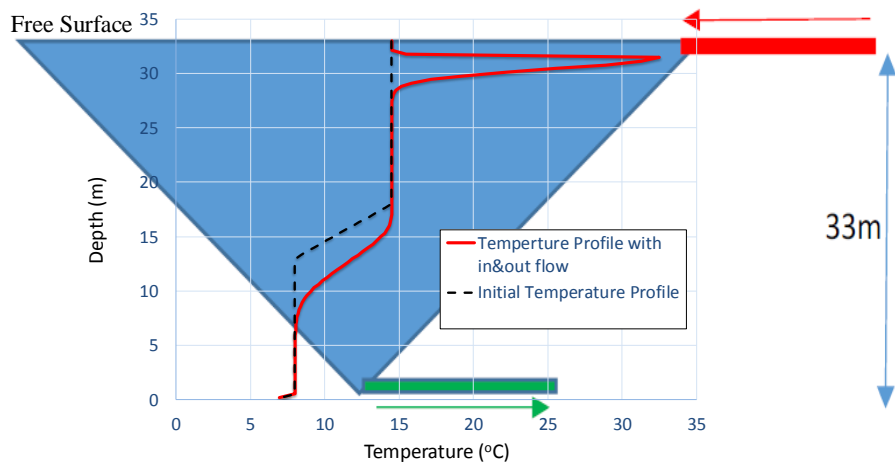


Figure 4.24: Temperature distribution when the inflow at the surface and the outflow at the bottom.

Case 1 is given in Figure 4.24. This might be the most realistic case when water release and withdrawal of nuclear power plant cooling systems are considered. Near the free surface temperature increases by $18.5\text{ }^{\circ}\text{C}$. Over the first 5m below free surface temperature changes quite abruptly. This is also influenced a change in thermocline. For instance, temperature of water initially at the depth 11 m is around $8\text{ }^{\circ}\text{C}$, after the release of hot water near the surface temperature at that location rises to $10.85\text{ }^{\circ}\text{C}$.

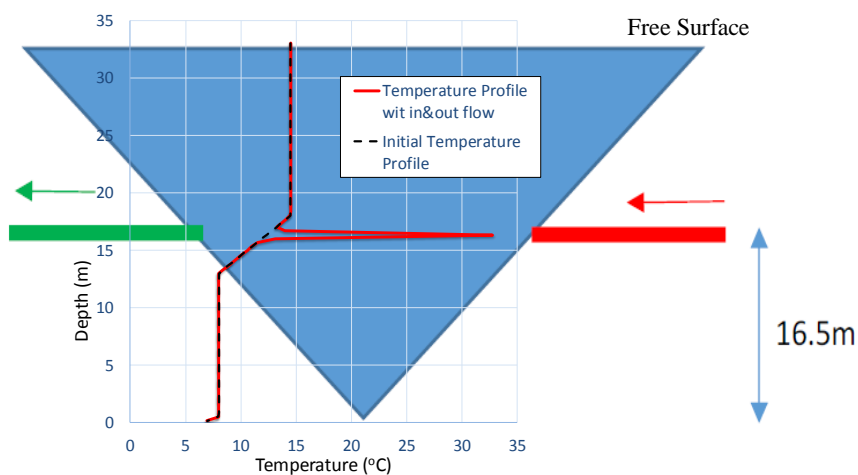


Figure 4.25: Temperature distribution when both the inflow and the outflow are at the mid-depth.

The second case shown in Figure 4.25 is not as realistic as the first case. The release and withdrawal of water occurs at the same depth. This option has a crucial impact at thermocline and it is undesirable in plant operation as the cooling water temperature might rise quite significantly. The abrupt temperature change happens in only 1 m depth on the thermocline.

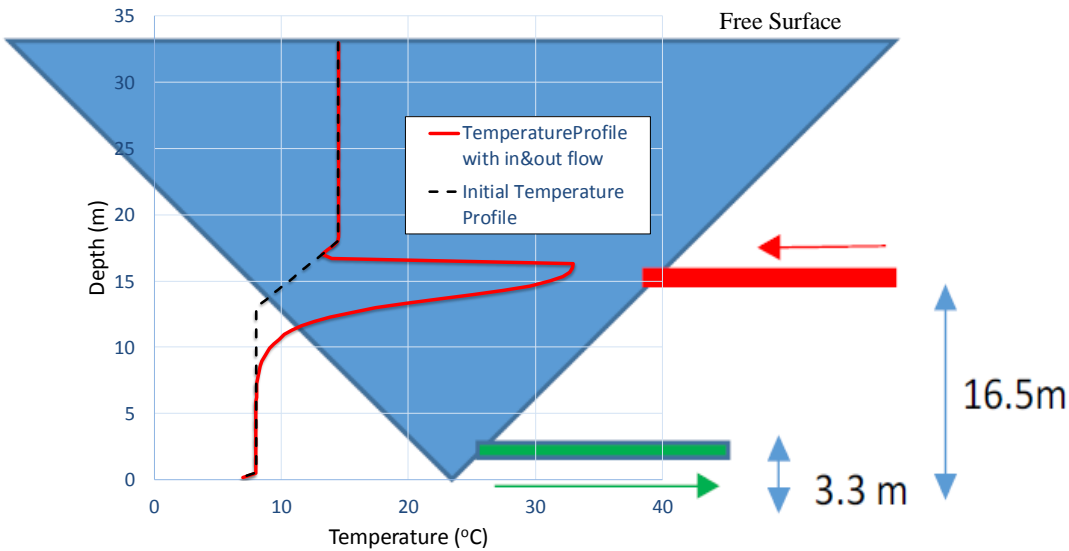


Figure 4.26: Temperature distribution when the inflow at the middle and outflow near the bottom

In the final case shown in Figure 4.26, the rapid increase in temperature at thermocline zone is harmful for lake habitat and the temperature variation is much wider in this case compared to the case given in Figure 4.25.

From Figures 24, 25 and 26 it is observed that inflow of the hot water causes a rapid change of temperature at and around its location.

4.3.2. Effect of Solar Radiation on Combined with Inflow and Outflow Cases

In this subsection, effects of short wave solar radiation are combined with the inflow and outflow effects on vertical temperature distribution of the water body. The position of inflow is at the half depth of the reservoir and the position of the outflow is almost near the bottom which is equal to 3.3 m from the lake bottom. Two magnitudes of short wave radiation such as 250 W/m^2 and 50 W/m^2 are considered as given in Figure 4.27. The simulation is done for 24 hours and the initial conditions are same with the cases in Section 4.3.1. Solar radiation takes a peak value at noon, the diurnal effect on solar radiation is considered using a sinusoidal variation. This variation is shown in the figure. Due to sunset the magnitude of solar radiation takes zero value.

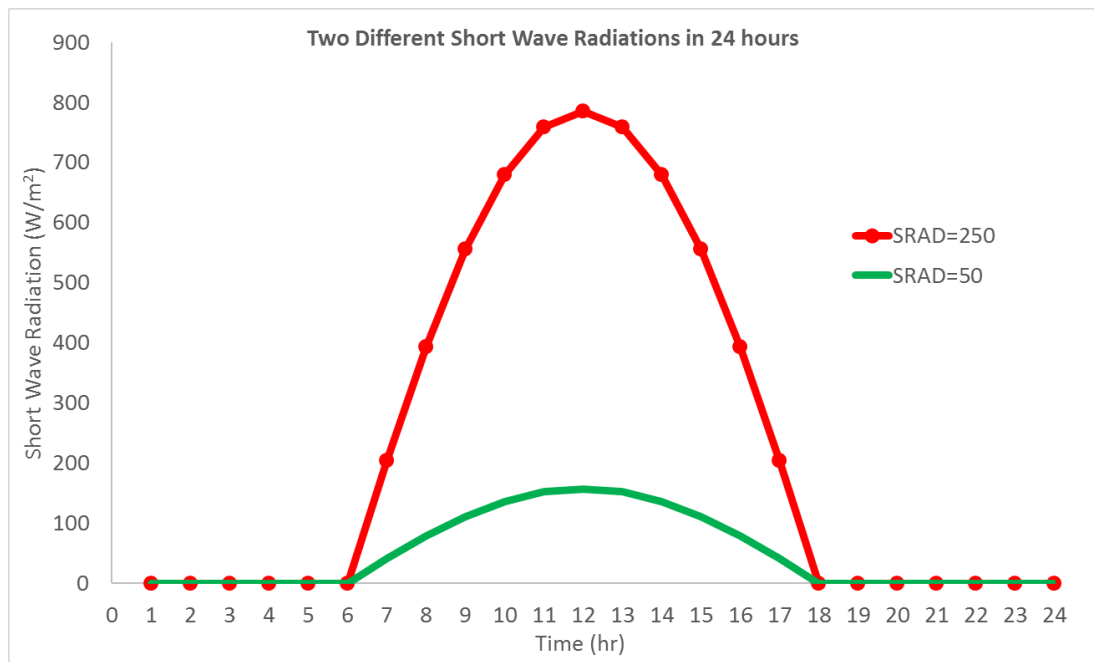


Figure 4.27: Sinusoidal variation of short wave radiation in 24 hours with two different magnitudes of SRAD: 250 W/m^2 & 50 W/m^2

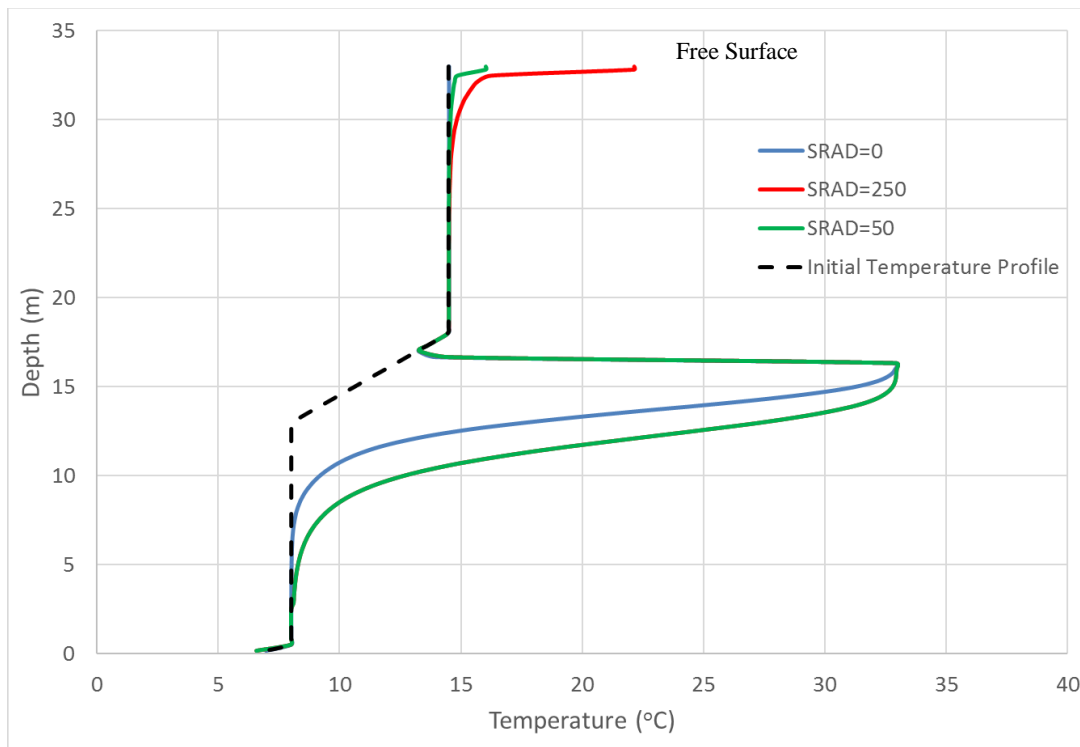


Figure 4.28: Temperature distribution when the inflow at the middle and outflow near the bottom combined with different solar radiation magnitudes.

Short wave radiation affects the surface of the water body mostly. As shown in Figure 4.28, when solar radiation is considered, the high temperature zone shifted down increasing the depth over which the higher temperature values are observed. When shortwave radiation is equal to 250 W/m^2 , surface water temperature is almost at 23°C and for 50 W/m^2 shortwave radiation, surface water temperature is at 16°C .

Figure 4.29 is equivalent to case 1, however here solar radiation is taken into account with $\text{SRAD} = 250 \text{ W/m}^2$ of the free surface. This figure shows with conservative SRAD of 250 W/m^2 , which produces maximum short wave radiation at noon around 800 W/m^2 , free surface temperature could reach up to 34°C with hot water release. This also significantly affects the full vertical profile causing an overall increase in temperature even close to lake bottom.

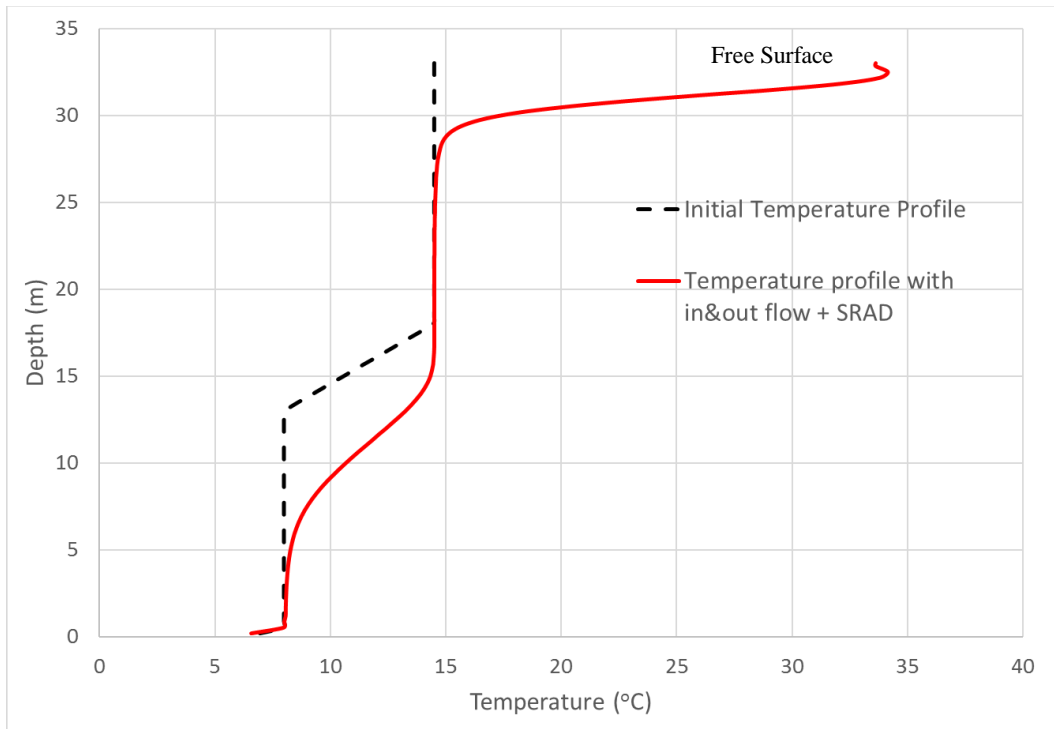


Figure 4.29: Temperature distribution when the inflow at the surface and outflow near the bottom combined with 250 W/m^2 solar radiation.

4.3.3. Effect of Melted Snow Water as a Surface Inflow

In this chapter, temperature profile of 30th of April in figure 4.2 is used to observe cooling effect of melting water at the surface which can cause a turnover phenomenon if combined with the surface wind's mechanical effect. As mentioned in section 4.1.4, by surface cooling an unstable stratification occurs.

On 30th of April, the temperature near the bottom is about $6.5 \text{ }^\circ\text{C}$ and near the surface is about $7.2 \text{ }^\circ\text{C}$. The heat flux of these temperature are calculated below, and provided as an input to the code.

$$\text{VST1}(3) = [^\circ\text{C}] \times [\rho] \times [C_p]$$

$$\text{VST1}(3) = 6.5 \times 1000 \times 4185.5 = 2.72 \times 10^7 \text{ J/m}^3 \quad z = 1\text{m}$$

$$\text{VST2}(3) = 7.2 \times 1000 \times 4185.5 = 6.07 \times 10^7 \text{ J/m}^3 \quad z = 32\text{m}$$

Melting water is assumed to be at +1 °C, which is mixed with surface water of the lake. Surface heat flux used in the code is given as;

$$\text{Heat Flux} = 1 \times 1000 \times 4185.5 = 0.41 \times 10^7 \text{ J/m}^3$$

The simulation time is 24 hours and the heating effect from solar radiation is neglected to see the pure effect of inflow of melting snow. Time step is taken as 1 minute. Temperature profile within the lake after 24 hours is given in figure 4.30.

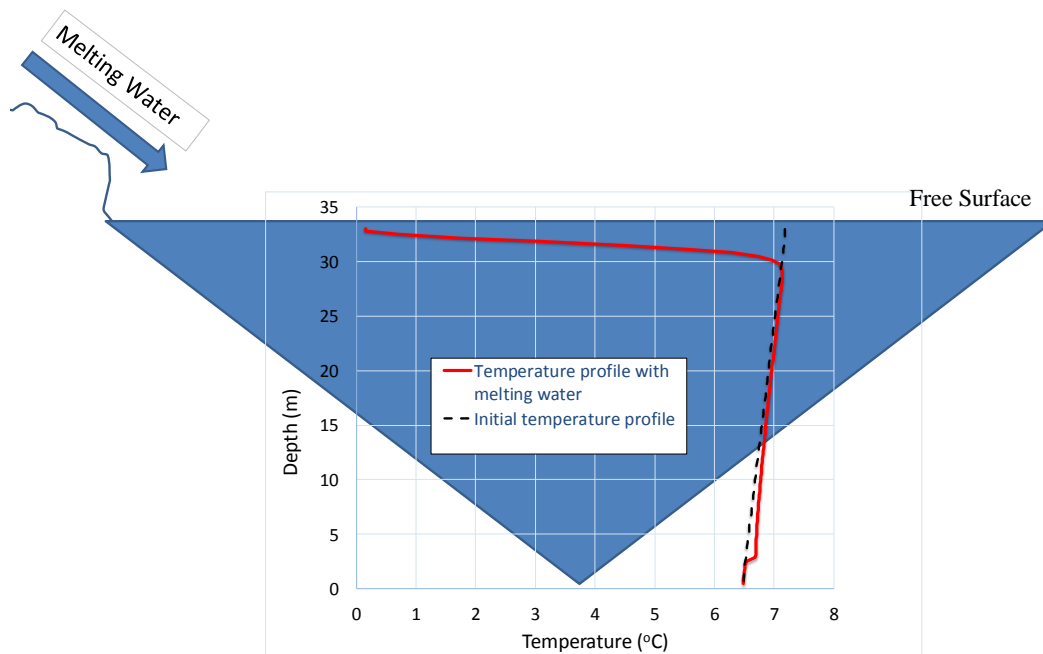


Figure 4.30: Temperature distribution as the melting water is considered as inflow to the lake.

CHAPTER 5

CONCLUSION

Vertical temperature distribution in a lake is a crucial for engineers, ecologists and geomorphologists. The main components that affect this distribution are wind effects, solar radiation, seasonal heating/cooling and inflow/outflows. Wind effect is the main mechanical effect that drive the mixing process. Summer formation of thermocline is quite possible in lakes in Northern Hemisphere.

In this study, real data of Llyn Cwelly North Wales (Darbyshire and Edwards, 1972) applied to an artificial lake by taking nuclear power plant cooling scenarios to consideration. Releasing of the hot water to a lake or a man-made pool has important results on the vertical temperature profile in terms of the quality of water and habitat of living organisms. Forecasting the rapid change of temperature by using PROBE might offer a significant advantage before designing cooling systems of such plants. In PROBE, simulation of 24 hours-period takes few minutes, therefore finding a solution to a problem or optimization of the solution in a very short time interval is the strongest point of the code. Furthermore; numerical modelling eliminates hampering of scale effects of laboratory experiments of such phenomenon.

In our study we found that,

- i) Wind conditions affect the overall velocity and mixing conditions in a lake.
- ii) Bathymetry of a lake might affect the mixing process.

- iii) For realistic results Coriolis' effects should be considered.
- iv) Solar radiation is an important input in thermal studies of lakes.
- v) Release location of hot water combined with solar radiation must be studied for nuclear plants considered in order to gain insight of possible outcomes of cooling systems of such facilities.

5.1. Future Works

Real operation scenarios of designed nuclear plant in Turkey could be simulated in conjunction with solar radiation research. By running many scenarios optimization studies are also possible.

The concentrations of possible constituents in lake water can be considered in the code. Their change with temperature, if any, could be evaluated.

The effects of waves on the surface and roughness at the bottom of the lake can be taken into consideration in simulations.

In this study, one-dimensional code is used. Further information of many processes could be achieved by using higher dimensional models to study thermal effects of lakes.

This code allows changes in the free surface elevation, if unequal inflow and outflow conditions to and from a reservoir exist. Therefore, it is also possible to study scenarios of uneven withdrawal and influx. However, water overflow is not allowed from the reservoir numerically.

REFERENCES

- Aksoy, B. (2011) Solar Radiation over Turkey and Its Analysis, International Journal of Remote Sensing. Turkish State Meteorological Service, Research Department, Ankara, Turkey
- Boehrer, B. and Schultze, M. (2008) Stratification of Lakes. *Reviews of Geophysics* **46**, The American Geophysical Union, 1-27.
- Çağlar, A., Yamalı, C., Baker, D. K., Kaftanoğlu, B. (2012) Measurement of Solar Radiation in Ankara, Turkey, *Journal of Thermal Science and Technology* **33**, Middle East Technical University, Akdeniz University, Atılım University. 135-142.
- Çalışkan, A. & Elçi. Ş. (2009) Effects of Selective Withdrawal on Hydrodynamics of a Stratified Reservoir. *Water Resource Manage*, **23**, 1257-1273.
- Darbyshire, J. and Edwards, A. (1972) Seasonal Formation and Movement of the Thermocline in Lakes. *Formation and movement of the Thermocline*, **93**, Marine Science Laboratories, U.K.
- Elliott, J. A., Persson, I., Thackeray, S. J. and Blenckner, T. (2007) Phytoplankton modelling of Lake Erken, Sweden by linking the models PROBE and PROTECH, *Ecological Modelling*, **202**, 421-426.
- Gal, G., Imberger, J., Zohary, T., Antenucci, J., Anis, A. and Rosenberg, T. (2003) Simulating the thermal dynamics of Lake Kinneret. *Ecological Modelling* **162**, University of Western Australia, 69-86.
- Hambright K.D. (1994) Can zooplanktivorous fish really affect lake thermal dynamics? *Archiv für Hydrobiologie*, **130**, 429-438.

- Hamilton, D. P. And Schladow, S. G. (1997) Prediction of Water Quality in Lakes and Reservoirs. Part 1- Model Description. *Ecological Modelling* **96**, University of Western Australia, Australia, 91-110.
- Hocking G.C. & Straskraba M. (1999) The effect of light extinction on thermal stratification in reservoirs and lakes. *International Review of Hydrobiology*, **84**, 535–556.
- Horne, A. & Goldman, C. (1994) Limnology, *McGraw-Hill Key Textbooks Series.*, New York, 480 p.
- Hornung, R. (2002) Numerical modelling of stratification in Lake Constance with the 1-D hydrodynamic model DYRESM. M.S. thesis. Univ. of Stuttgart, Germany.
- Hutchinson G.E. (1957) A Treatise on Limnology, Vol. 1. Geography, Physics, and Chemistry, John Wiley & Sons Inc., New York.
- Imberger, J. (1982) Reservoirs dynamics modelling. In: E.M. O’Laughlin and P. Cullen (Editors), Predictions in Water Quality. Aust. Acad. Sci., Canberra, 223-248.
- Imboden, D. M. and Wüest, A. (1995) Mixing Mechanism in Lakes. *Environmental Physics* **4**, Switzerland, 83-138.
- Jones I., George G. & Reynolds C. (2005) Quantifying effects of phytoplankton on the heat budgets of two large limnetic enclosures. *Freshwater Biology*, **50**, 1239-1247.
- Jones, I., Sahlberg, J. and Persson, I. (2010) Modelling the Impact of Climate Change on the Thermal Characteristics of Lakes. *The Impact of Climate Change on European Lakes* **4**, Springer Science + Business Media B.V., U.K., 103-120.

- Kirillin, G. (2010). Modeling the impact of global warming on water temperature and seasonal mixing regimes in small temperate lakes. *Boreal Environ. Res.* **15** (2), 279–293.
- Kirillin, G. and Shatwell, T. (2016) Generalized Scaling of Seasonal Thermal Stratification in Lakes. *Earth-Science Reviews* **161**, Department of Ecohydrology, Germany, 179-190.
- Kling G. (1988) Comparative transparency, depth of mixing and stability of stratification in lakes of Cameroon, West Africa. *Limnology and Oceanography*, **33**, 27–40.
- Kraus, E. B. and Turner, J. S. (1967) A one-dimensional model of the seasonal thermocline. *Tellus* **19**, Woods Hole Oceanographic Institution, Massachusetts.
- MacIntyre, S., Flynn, K. M., Jellison, R. and Romero, J. R. (1999) Boundary mixing and nutrient fluxes in Mono Lake, California. *Limnology and Oceanography* **44**, the American Society of Limnology and Oceanography, 512-529.
- Mazumder A. & Taylor W. (1994) Thermal structure of lakes varying in size and water clarity. *Limnology and Oceanography*, **39**, 968–976.
- Mazumder A., Taylor W.D., McQueen D.J. & Lean D.R.S (1990) Effects of fish and plankton on lake temperature and mixing depth. *Science*, **247**, 312–315.
- Omstedt, A., Chen, Y. and Wesslander, K. (2005) A comparison between the ERA40 and the SMHI gridded meteorological databases as applied to Baltic Sea modelling. *Hydrology Research*, **36**, 369-380.
- Omstedt, A. and Svensson, U. (1984) Modelling super cooling and ice formation in a turbulent Ekman layer. *Journal of Geophysical Research*, **89**, 735-744.
- Owens, E. M. (1998) Development and Testing of One-Dimensional Hydrothermal Models of Cannonsville Reservoir. *Journal of Lake and Reservoir*

- Management* **14**, the North American Lake Management Society, Syracuse University, 172-185.
- Perroud, M., Goyette, S., Martynov, A., Beniston, M. and Anneville, O. (2009) Simulation of multiannual thermal profiles in deep Lake Geneva: A comparison of one-dimensional lake models. *Limnology and Oceanography* **54**, the American Society of Limnology and Oceanography, 1574-1594.
- Persson, I. and Jones, I. D. (2008) The Effect of Water Colour on Lake Hydrodynamics: A Modelling Study. *Freshwater Biology* **53**, Uppsala University, Sweden, 2345-2355.
- Quay, P. D., Broecker, W. S., Hesslein, R. H., and Schindler, D. W. (1980) Vertical diffusion rates determined by tritium tracer experiments in the thermocline and hypolimnion of two lakes. *Limnology and Oceanography* **25**, the American Society of Limnology and Oceanography, 201-218.
- Romero, J. R., Antenucci, J.P. and Imberger, J. (2004) One and three-dimensional biogeochemical simulations of two differing reservoirs. *Ecological Modelling* **174**, University of Western Australia, Australia, 143-160.
- Sahlberg, J. (1983) A Hydrodynamical Model for Calculating the Vertical Temperature Profile in Lakes During Cooling. *Hydrology Research*, **14**, 239-254.
- Sahlberg, J. (2003) Physical Modelling of the Akkajaure reservoir. *Hydrology and Earth System Sciences*, **7**, Swedish Meteorological and Hydrological Institute, Sweden, 268-282.
- Schindler, D.W., Bayley, S.E., Parker, B.R., Beaty, K.G., Cruikshank, D.R., Fee, E.J., Schindler, E.U. & Stainto, M.P. (1996) The effects of climatic warming on the properties of boreal lakes and streams at the experimental lakes area, northwestern Ontario. *Limnology and Oceanography*, **41**, 1004–1017.

- Shatwell, T., Adrian, R., Kirillin, G. (2016). Planktonic events may cause polymictic-dimictic regime shifts in temperate lakes. *Sci. Report.* **6**, 24361.
- Socolofsky, S. A. and Jirka, G. H. (2004) Mixing in Lakes and Reservoirs.
- Spigel, R. H. and Imberger, J. (1980) The Classification of Mixed-Layer Dynamics in Lakes of Small to Medium Size. *Journal of Physical Oceanography*, **10**, American Meteorological Society, 1104-1121.
- Svensson, U. (1978) A mathematical model of the seasonal thermocline dept. of Water Resources Eng., Univ. of Lund, Sweden, Report No.1002.
- Svensson, U. (1979) The Structure of the Turbulent Ekman Layer. *Tellus* **31**, University of Lund, Sweden, 340-350.
- Svensson, U. (1986) PROBE an instruction manual, *The Swedish Meteorological and Hydrological Institute*, S-601 76 Norrköping, Sweden.
- Tucker, W. A. and Green, A. W. (1977) A Time-Dependent Model of the Lake-Averaged, Vertical Temperature Distribution of Lakes. *Limnology and Oceanography*, **22**, 687-699.
- Web 1, Thermal Stratification. (2012). Retrieved June 19, 2017, from http://msue.anr.msu.edu/news/the_thermocline_a_summer_phenomenon_in_michigan_inland_lakes
- Web 2, The Doel Nuclear Power Station. (n.d.). Retrieved June 18, 2017, from <http://corporate.engie-electrabel.be/local-player/nuclear-3/>
- Web 3, Once-through Cooling Systems. (n.d.). Retrieved June 18, 2017, from <http://www.crystal lagoons.com/industrial-applications/>
- Web 4, A Remotely Sensed Image Showing The Effects Of Thermal Pollution (*Eurosense–Maasvlakte Project, Netherlands*). (n.d.). Retrieved March 8, 2017, from <http://www.eurosense.com/documents/graphics/images/your->

application/watermanagement/hot_water_distribution_maasvlakte_eurosense
_b.jpg

Web 5, Historic Temperature, Rain and Sun Hour Data for Valley, North Wales. (n.d.). Retrieved May 10, 2017, from <http://www.metoffice.gov.uk/public/weather/climate/historic/#?tab=climateHistoric>

Web 6, Coriolis Frequency Calculator. (2000). Retrieved from March 8, 2017, <https://www.mt-oceanography.info/Utilities/coriolis.html>

Web 7, Beaufort Scale. (n.d.). Retrieved from July 6, 2017, <https://www.rmets.org/weather-and-climate/observing/beaufort-scale>

Weinstock, J. (1981) Vertical turbulence diffusivity for weak or strong stable stratification. *J. Geophys. Res.*, **86**, 9925-9928.

Yan, N.D. & Dillon P.J. (2000) Zooplankton biomass rarely improves predictions of chlorophyll concentration in Canadian Shield lakes that vary in pH. *Aquatic Ecology*, **34**, 127–136.

Yeates, P. S. (2008) Deep Mixing in Stratified Lakes and Reservoirs, Thesis of Doctor of Philosophy, University of Western Australia, Australia.